AD-A123 517 AIR MASS TRAJECTORIES AND ATMOSPHERIC RADON MEASUREMENTS DURING THE EOMET..(U) PACIFIC MISSILE TEST CENTER POINT MUGU CA T E BATTALINO ET AL. NOV 82 1/1

UNCLASSIFIED PMTC-TP-000001 F/G 4/2 NL

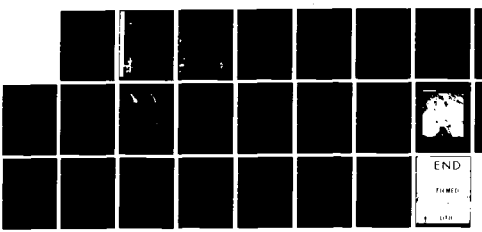

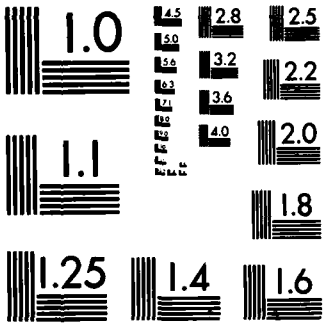

(2)

Technical Publication TP000001

AIR MASS TRAJECTORIES AND ATMOSPHERIC RADON MEASUREMENTS DURING THE EOMET/OSP EXPERIMENTS ON SAN NICOLAS ISLAND (1978-1980)

(PREPARED FOR ELECTRO-OPTICAL METEOROLOGY (EOMET) PROGRAM, NAVAL OCEAN SYSTEMS CENTER)

By

T. E. BATTALINO
and
R. A. HELVEY

Geophysics Division

NOVEMBER 1982

PACIFIC MISSILE TEST CENTER

Point Mugu, California 93042

PACIFIC MISSILE TEST CENTER

AN ACTIVITY OF THE NAVAL AIR SYSTEMS COMMAND

This report was prepared for the Electro-Optical Meteorology (EOMET) Program, Naval Ocean Systems Center.

Mr. J. Rosenthal, Head, Geophysics Sciences Branch; Mr. D. A. Lea, Associate Geophysics Officer; and Mr. C. G. Elliott, Project Manager, have reviewed this report for publication.

K. I. LICHTI
Technical Director

Technical Publication TP000001

Published by . . . . . Information Technology Department
Security classification . . . . . UNCLASSIFIED
First printing . . . . . 150 [illegible]

UNCLASSIFIED

SECURITY CLASSIFICATION OF THIS PAGE *(When Data Entered)*

REPORT DOCUMENTATION PAGE		READ INSTRUCTIONS BEFORE COMPLETING FORM
1. REPORT NUMBER TP000001	2. GOVT ACCESSION NO. AD-A123517	3. RECIPIENT'S CATALOG NUMBER
4. TITLE *(and Subtitle)* AIR MASS TRAJECTORIES AND ATMOSPHERIC RADON MEASUREMENTS DURING THE EOMET/OSP EXPERIMENTS ON SAN NICOLAS ISLAND (1978-1980)		5. TYPE OF REPORT & PERIOD COVERED 6. PERFORMING ORG. REPORT NUMBER
7. AUTHOR(s) T. Battalino and R. Helvey		8. CONTRACT OR GRANT NUMBER(s)
9. PERFORMING ORGANIZATION NAME AND ADDRESS Pacific Missile Test Center Point Mugu, California 93042		10. PROGRAM ELEMENT, PROJECT, TASK AREA & WORK UNIT NUMBERS
11. CONTROLLING OFFICE NAME AND ADDRESS Naval Air Systems Command Washington, DC 20361		12. REPORT DATE November 1982 13. NUMBER OF PAGES 23
14. MONITORING AGENCY NAME & ADDRESS*(if different from Controlling Office)*		15. SECURITY CLASS. *(of this report)* UNCLASSIFIED 15a. DECLASSIFICATION/DOWNGRADING SCHEDULE

16. DISTRIBUTION STATEMENT *(of this Report)*

Approved for public release; distribution unlimited.

17. DISTRIBUTION STATEMENT *(of the abstract entered in Block 20, if different from Report)*

18. SUPPLEMENTARY NOTES

19. KEY WORDS *(Continue on reverse side if necessary and identify by block number)*

Air mass trajectory	Electro-optical propagation
Atmospheric radon	Maritime aerosols
Coastal aerosols	SNI electro-optical studies

20. ABSTRACT *(Continue on reverse side if necessary and identify by block number)*

The characteristic properties and evolutionary processes of naturally occurring and man-made aerosols is a subject of considerable importance for modeling electro-optical propagation through the atmosphere. The Navy's effort is centered upon predicting propagation conditions that impact on sensor and communication systems in the marine environment. Since the aerosol properties of an air mass depend primarily upon its source region and upon the alteration it undergoes in transit to the observation site, effective methods for air mass tracing are essential for modeling the atmospheric-optical environment. A series of five electro-optical field programs conducted at San Nicolas Island (1978-1980) afforded an opportunity to compare two independent methods for identifying

DD FORM 1 JAN 73 1473 EDITION OF 1 NOV 65 IS OBSOLETE

UNCLASSIFIED

SECURITY CLASSIFICATION OF THIS PAGE *(When Data Entered)*

20. ABSTRACT *(Concluded)*

air mass regimes. One technique utilized measurements of atmospheric radon concentrations as an air mass tracer while the other approach employed a computerized objective analysis scheme to automatically construct surface air trajectories. The categorization of over 270 trajectories into low (<10 pCi/m^3), medium (≥10, <30 pCi/m^3), and high (≥30 pCi/m^3) radon concentrations provides an approximate description of the air parcel history for these conditions.

ACKNOWLEDGEMENT

The authors gratefully acknowledge the generous assistance of Dr. R. E. Larson for several informative discussions concerning atmospheric radon. We are also indebted to S. G. Gathman for supplying the radon data, and to J. Rosenthal and D. A. Lea for providing helpful comments and suggestions. In addition, we express our appreciation to Dr. J. Richter of NOSC, the project sponsor, for his encouragement and support.

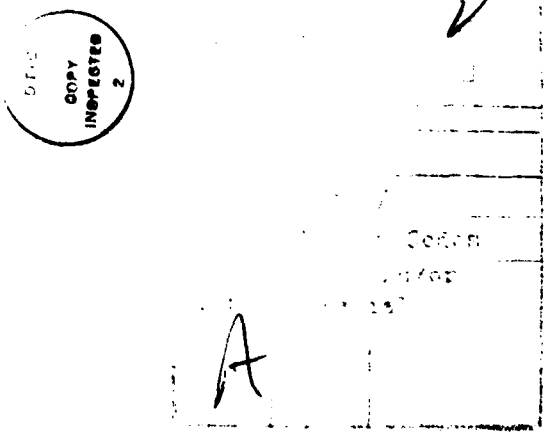

CONTENTS

	Page
SUMMARY	1
1. INTRODUCTION	3
2. ATMOSPHERIC RADON	5
3. TRAJECTORY ANALYSIS TECHNIQUE	6
4. COMPARISON OF AIR TRAJECTORIES AND RADON LEVELS	7
5. SYNOPTIC CONDITIONS AND RADON LEVELS	13
a. May 1978	13
b. November 1978	13
c. April/May 1979	13
d. January 1980	16
e. July 1980	16
6. RADON VERSUS INVERSION ALTITUDE	16
7. RADON VERSUS AIR PARCEL SPEED	18
8. PSEUDO MEAN RADON DISTRIBUTION	18
9. CONCLUSIONS	18
REFERENCES	21
TABLES	
1. Station Locations Used in Trajectory Computations	8
2. Trajectory/Radon Sample Size for Radon Concentration Categories During Each of the Five Experiments	8
FIGURES	
1. Southern California Coastline and the Offshore Islands	4
2. San Nicolas Island and the Marine Environment Test Range (METR)	4
3. Air trajectories ending at SNI for all measurement periods are illustrated with their resolution into the low (<10 pCi/m^3), medium ($\geq 10, <20$ pCi/m^3), and high (≥ 30 pCi/m^3) radon categories. Note the trajectory paths "filling in" the southern California bight area as the radon concentration category increases	9
4. Air trajectories terminating at SNI during each measurement experiment are illustrated for the low (<10 pCi/m^3) radon category. In general, low radon levels measured at SNI are associated with a mostly overwater northwesterly to westerly trajectory pattern	10

CONTENTS (Concluded)

Page

FIGURES (Continued)

5. Air trajectories ending at SNI during each measurement experiment are illustrated for the high ($\geq$30 pCi/m^3) radon category. High radon levels were not observed during the last experiment (July 1980). In general, high radon levels measured at SNI are associated with air trajectories that have a history over land or in the southern California bight 11
6. Air trajectories terminating at SNI during each measurement experiment are illustrated for the medium ($\geq$10, $<$30) radon category. These maps exhibit trajectory paths that are similar to those found in both the low and high radon concentration categories and are suggestive of a transition mode 12
7. GOES Satellite Imagery at 1845Z (1045 PST) – 14 May 1978. Catalina Eddy Engulfs Southern California Bight in Marine Stratus 14
8. Pacific Surface Weather Analysis Charts for Selected Periods During the EOMET/OSP Experiments (1978-1980) on SNI. 15
9. Scatter diagram shows relationship between radon concentration and the approximate altitude of the base of the marine inversion layer for available data during the five experiments. Figures 9(b)–9(e) illustrate trajectory paths isolated according to radon levels and inversion altitude 17
10. Radon concentration plotted against average wind speed for 12-hour trajectories during all measurement periods (figure 10a) and during the April/May 1979 experiment (figure 10b) 19
11. Plotted numbers and isopleths indicate average radon concentrations (measured at SNI) for 12-hour trajectories (ending at SNI) passing over the indicated areas. 20

Technical Publication TP000001
November 1982

PACIFIC MISSILE TEST CENTER
Point Mugu, California 93042

AIR MASS TRAJECTORIES AND ATMOSPHERIC RADON MEASUREMENTS DURING THE EOMET/OSP EXPERIMENTS ON SAN NICOLAS ISLAND (1978-1980)

(PREPARED FOR ELECTRO-OPTICAL METEOROLOGY (EOMET) PROGRAM, NAVAL OCEAN SYSTEMS CENTER)

By

Terry E. Battalino

and

Roger A. Helvey

SUMMARY

The characteristic properties and evolutionary processes of naturally occurring and man-made aerosols is a subject of considerable importance for modeling electro-optical propagation through the atmosphere. The Navy's effort is centered upon predicting propagation conditions that impact on sensor and communication systems in the marine environment. Since the aerosol properties of an air mass depend primarily upon its source region and upon the alteration it undergoes in transit to the observation site, effective methods for air mass tracing are essential for modeling the atmospheric-optical environment. A series of five electro-optical field programs conducted at San Nicolas Island (1978-1980) afforded an opportunity to compare two independent methods for identifying air mass regimes. One technique utilized measurements of atmospheric radon concentrations as an air mass tracer while the other approach employed a computerized objective analysis scheme to automatically construct surface air trajectories. The categorization of over 270 trajectories into low (<10 pCi/m^3), medium (≥ 10, <30 pCi/m^3), and high (≥ 30 pCi/m^3) radon concentrations provides an approximate description of the air parcel history for these conditions.

The lowest radon concentrations occurred when the air traversed a northwesterly to westerly oceanic path before ending at San Nicolas Island. The highest radon levels were associated with air parcels that either passed over land or through the southern California bight. In a few cases relatively high radon concentrations were observed for over-water trajectories, indicating earlier overland travel or horizontal/vertical mixing with continental air. The synoptic features and meteorological factors responsible for the observed results are discussed.

Publication UNCLASSIFIED.

1. INTRODUCTION

San Nicolas Island (SNI) is located off the southern California coast about 120 Km west-southwest of Los Angeles (figure 1) and is routinely used by the Navy's Pacific Missile Test Center as a weapons testing and radar tracking site. In a concerted effort to characterize the effects of a maritime atmosphere on optical and infrared transmission pertinent to weapons RDT&E, the U.S. Navy has established an atmospheric transmissometer and micrometeorological facility on the northwestern end of SNI (figure 2). Measurements began in 1978 under the sponsorship of the Navy's Electro-Optical Meteorology (EOMET) and Optical Signatures (OSP) programs. To date a total of five Atmospheric-Optical measurement programs have been conducted on SNI (Blanc, 1978[1], 1979[2], 1981[3], 1982[4]; Matthews et al., 1979[5]; Jeck, 1979[6]; Rosenthal et al., 1979[7]; Clark et al., 1981a[8], 1981b[9], 1982a[10], 1982b[11]).

One of the major objectives of the EOMET program is to characterize, for a variety of atmospheric conditions, the marine boundary layer meteorological parameters that influence electro-optical propagation. One approach in this endeavor is to derive meteorologically dependent aerosol models (e.g., Barnhardt and Streete, 1970[12]; Wells et al., 1977[13]; Katz et al., 1979[14]) from which extinction coefficients can be computed using Mie scattering theory. Since the refractive index of aerosol particles, which is required in Mie computations of aerosol extinction, depends primarily on air mass history (Richter and Hughes, 1981[15]), it is reasonable to attribute at least some of the marine aerosol model deficiencies encountered in validation efforts (Hughes and Richter, 1979[16]; Noonkester, 1980[17];

---

[1]Blanc, T. V., 1978: Micrometeorological data for the Cooperative Experiment for West Coast Oceanography and Meteorology (CEWCOM-78) at San Nicolas Island, California Vol. I and II. NRL Memorandum Report 3871, Aug. 1978. UNCLASSIFIED

[2]Blanc, T. V., 1979: Micrometeorological data report for the November 1978 Electro-Optics Meteorology (EOMET) experiment at San Nicolas Island, California. NRL Memorandum Report 4056, Aug. 1979. UNCLASSIFIED

[3]Blanc, T. V., 1981: Report and analysis of the May 1979 marine surface layer micrometeorological experiment at San Nicolas Island, California. NRL Report 8363, Dec. 1981. UNCLASSIFIED

[4]Blanc, T. V., 1982: The data base for the May 1979 marine surface layer micrometeorological experiment at San Nicolas Island, California. NRL Report 4713, May 1982. UNCLASSIFIED

[5]Matthews, G. B., B. E. Williams, A. Akkerman, J. Rosenthal, and R. de Violini, 1978: Atmospheric transmission and supporting meteorology in the marine environment at San Nicolas Island–semiannual report. PACMISTESTCEN Technical Report TP-79-19, Dec. 1978. UNCLASSIFIED

[6]Jeck, R. K., 1979: Aerosol particle size measurements at San Nicolas Island during CEWCOM-78. NRL Memorandum Report 3931, Mar. 1979. UNCLASSIFIED

[7]Rosenthal, J., T. E. Battalino, V. R. Noonkester, and H. Hendon, 1979: Marine/continental history of aerosols at San Nicolas Island during CEWCOM-78 and OSP III. PACMISTESTCEN Technical Publication TP-79-33, Apr. 1979. UNCLASSIFIED

[8]Clark, R., T. E. Battalino, R. Helvey, and J. Rosenthal, 1981a: Atmospheric conditions and airmass history at San Nicolas Island during the November 1978 EOMET/OSP experiment. PACMISTESTCEN Technical Publication TP-81-30, Dec. 1981. UNCLASSIFIED

[9]Clark, R., T. E. Battalino, and R. Helvey, 1981b: Atmospheric conditions and airmass history at San Nicolas Island during the 30 April-11 May 1979 EOMET/OSP experiment. PACMISTESTCEN Technical PublicationTP-81-33, Dec. 1981. UNCLASSIFIED

[10]Clark, R., T. E. Battalino, and R. Helvey, 1982a: Atmospheric conditions and airmass history at San Nicolas Island during the 14-25 January 1980 EOMET/OSP experiment. PACMISTESTCEN Technical Publication TP-82-21, May 1982. UNCLASSIFIED

[11]Clark, R., T. E. Battalino, and R. Helvey, 1982b: Atmospheric conditions and airmass history at San Nicolas Island during the 22-31 July 1980 EOMET/OSP experiment. PACMISTESTCEN Technical Publication TP-82-22, May 1982. UNCLASSIFIED

[12]Barnhart, E. A., and J. L. Streete, 1970: A method for predicting atmospheric aerosol scattering coefficients in the infrared. Applied Optics, 9, 1337-1344. UNCLASSIFIED

[13]Wells, W. C., G. Gal, and M. W. Munn, 1977: Aerosol distributions in maritime air and predicted scattering coefficients in the infrared. Appl. Opt., 16, 654-659. UNCLASSIFIED

[14]Katz, B. S., K. Hepfer, and N. E. MacMeekin, 1979: Electro-optics meteorological sensitivity study. NSWC TR-79-67, Apr. 1979. UNCLASSIFIED

[15]Richter, J. H., and H. G. Hughes, 1981: Electro-optical atmospheric transmission effort in the marine environment. NOSC Technical Report 696, May 1981. UNCLASSIFIED

[16]Hughes, H. G., and J. H. Richter, 1979: Extinction coefficients calculated from aerosol size distributions measured in a marine environment. Proceedings of the Society of Photo-Optical Instrumentation Engineers, San Diego, CA., Aug. 29-30, 1979. UNCLASSIFIED

[17]Noonkester, V. R., 1980: Offshore aerosol spectra and humidity relations near southern California. Second Conference on Coastal Meteorology, Los Angeles, CA., Jan. 30-Feb. 1, 1980. UNCLASSIFIED

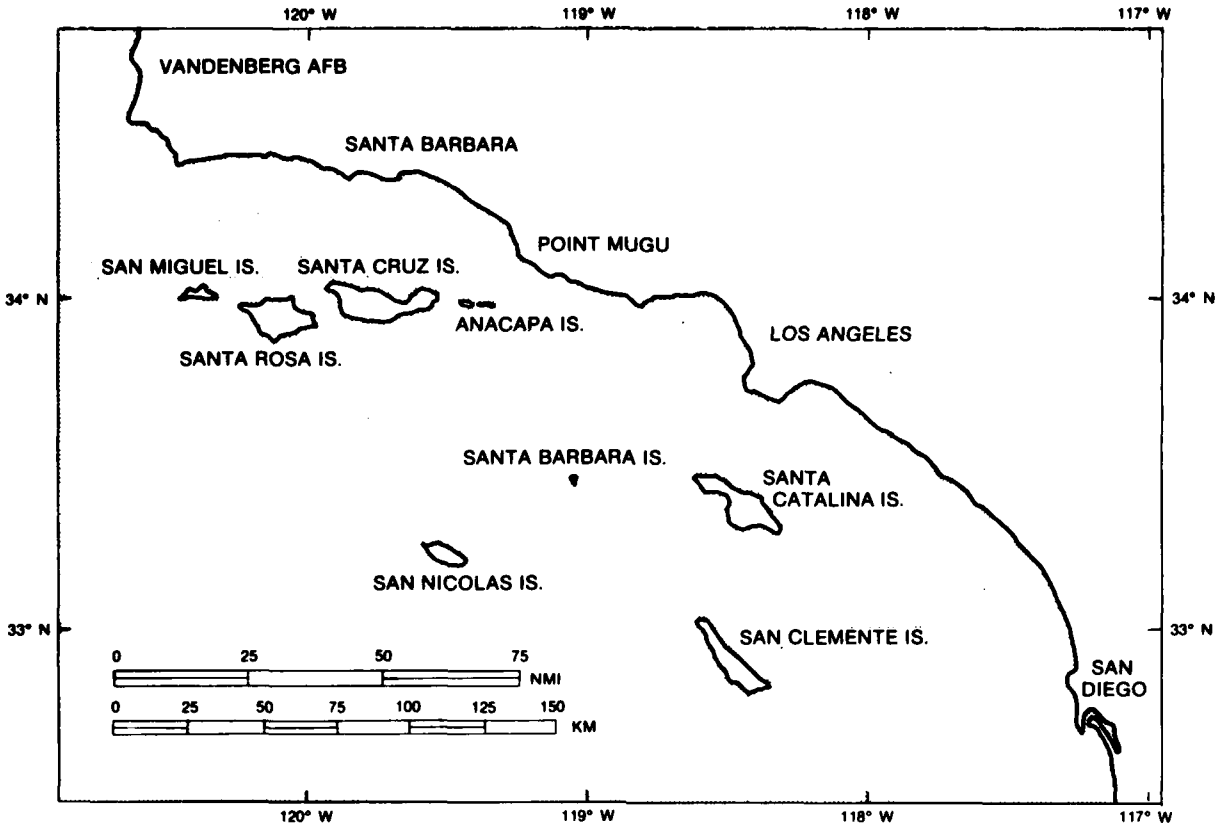

Figure 1. Southern California Coastline and the Offshore Islands.

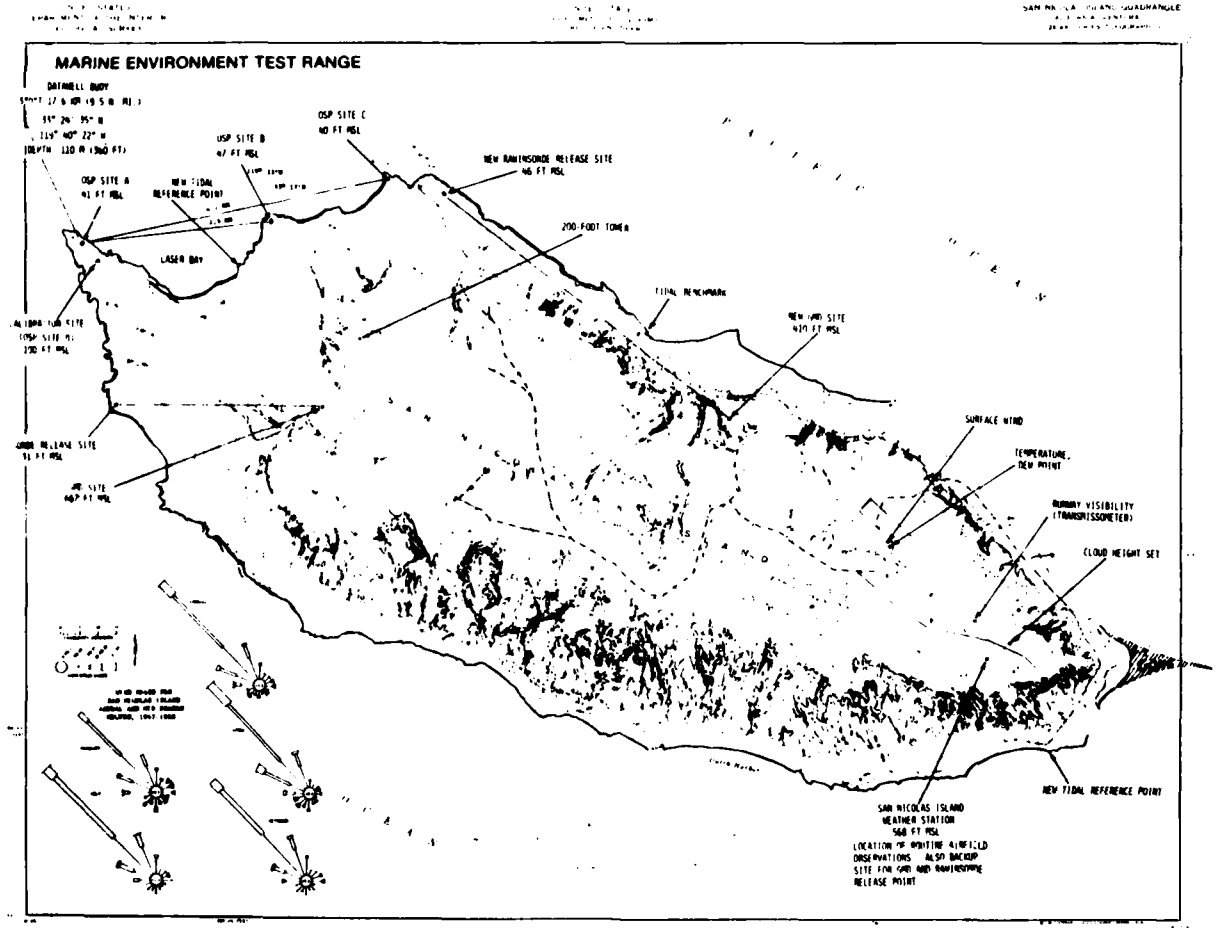

Figure 2. San Nicolas Island and the Marine Environment Test Range (METR).

Hughes, 1980[18]) to air mass differences. The next generation of marine aerosol models, such as the "Navy Model" (Gathman, 1982[19]), will explicitly incorporate air mass effects.

Two independent methods for characterizing air mass regimes were utilized during the EOMET/OSP measurements at SNI. One technique constructed surface air trajectories for parcels terminating at SNI, and the other approach measured the concentration of atmospheric radon gas for use as an air mass tracer. The purpose of this report is to compare these two air mass identification techniques and to discuss some of the related meteorological factors.

2. ATMOSPHERIC RADON

Radon 222, a product of the uranium 238 decay series, is an inert radioactive gas (half life 3.82 days) produced by the decay of radium 226 (half life 1622 years) which is found in various quantities in the so nd rocks of the earth's crust. Most of the rare gas emanates from continental areas, with less than 2% originati the oceans (Wilkening and Clements, 1975[20]). After formation in the ground, radon diffuses into the atmo re where its short lived daughter products become attached to aerosol particles that are transported with the p ng winds. The majority of the radon burden collected by an air mass depends upon its duration over land ns and the radon emissions rate from those regions; the removal processes are governed by radioactive decay, di and turbulent mixing (Larson et al., 1979c[21]). Because radon is produced mainly on land masses and has a ong half life, it has been widely used as an air mass tracer over oceanic areas (Fontan et al., 1963[22]; Vilenskii et al., 1967[23]; Rama, 1970[24]; Prospero and Carlson, 1970[25]; Wilkniss et al., 1974[26]; Moore et al., 1974[27]; Subramanian et al., 1977[28]; Larson, 1978[29], 1979b[30]; Larson et al., 1979[31]; Larson and Bressan, 1980[32]; Larson and Jeck, 1981[33]).

---

[18]Hughes, H. G., 1980: Aerosol extinction coefficient variations with altitude at 3.75 μm in a coastal marine environment. J. Appl. Meteor., 19, 803-808. UNCLASSIFIED

[19]Gathman, S. G., 1982: Navy aerosol model. Paper presented at the Annual Review Conference on Atmospheric Transmission Models, AFGL, Hanscom AFB, Mass., May 18-19, 1982. UNCLASSIFIED

[20]Wilkening, M. H. and W. E. Clements, 1975: Radon 222 from the ocean surface. J. Geophs. Res., 80, 3828-3830. UNCLASSIFIED

[21]Larson, R. E., D. J. Bressan, K. W. Marlow, T. A. Wojciechowski, and J. L. Heffter, 1979c: A comparison of concentrations of fission products, Radon 222, and cloud condensation nuclei over the North Atlantic. Pageoph., 117, 874-882. UNCLASSIFIED

[22]Fontan, J., D. Blanc, and A. Bouville, 1963: Meteorological conditions dependance of radon concentrations in air above the Atlantic. Nature, 197, 583-584. UNCLASSIFIED

[23]Vilenskii, V. D., G. V. Dmitrieva, and Yu. Kirasnopovtrev, 1967: Natural and artificial radioactivity of the atmosphere over the ocean and its relation to meteorological factors. U.S. Atomic Energy Commission Report AEC-TR-6711. UNCLASSIFIED

[24]Rama, K., 1970: Using natural radon for delineating monsoon circulation. J. Geophys. Res., 75, 2227-2229. UNCLASSIFIED

[25]Prospero, J. M., and T. N. Carlson, 1970: Radon-222 in the North Atlantic Trade Winds: its relationship to dust transport from Africa., Science, 167, 974-977. UNCLASSIFIED

[26]Wilkniss, P. E., R. E. Larson, D. J. Bressan, and J. Steranka, 1974: Atmospheric and continental dust near the antarctic and their correlation with air mass trajectories computed from Nimbus 5 satellite photographs. J. Appl. Meteor., 13, 512-515. UNCLASSIFIED

[27]Moore, H. E., S. E. Poet, E. A. Martell, and M. H. Wilkening, 1974: Origin of 222 Rn and its long-lived daughters in air over Hawaii. J. Geophys. Res., 79, 5019-5024. UNCLASSIFIED

[28]Subramanian, S. K., C. Rangarajan, S. Gopalakrishnan, and C. D. Eapen, 1977: Radon daughter's radioactivity levels over the Arabian Sea as indicators of air mass mixing. J. Appl. Meteor., 16, 487-492. UNCLASSIFIED

[29]Larson, R. E., 1978: Radon 222 measurements during marine fog events off Nova Scotia. J. Geophys. Res., 83, 415-418. UNCLASSIFIED

[30]Larson, R. E., 1979b: Atmospheric 222 Rn measurements at San Nicolas Island. NRL Technical Memorandum Report 4099, Nov. 1979. UNCLASSIFIED

[31]Larson, R. E., W. Kasemir, and D. J. Bressan, 1979: Measurements of atmospheric 222 Rn at San Nicolas Island and over nearby California coastal areas during CEWCOM-78. NRL Technical Memorandum Report 3941, Mar. 1979. UNCLASSIFIED

[32]Larson, R. E., D. J. Bressan, 1980: Air mass characteristics over coastal areas as determined by radon measurements. Second conference on Coastal Meteorology, Los Angeles, CA., Jan. 30-Feb. 1, 1980. UNCLASSIFIED

[33]Larson, R. E., and R. K. Jeck, 1981: Atmospheric 222 Rn measurements at San Nicolas Island during 1980. NRL Technical Memorandum Report 4649, Oct. 1981. UNCLASSIFIED

Relative changes in radon concentration are more meaningful as an atmospheric tracer than the absolute concentration (Larson et al., 1979[31]). This is true because the factors affecting radon exhalation depend upon the variable conditions of soil moisture (Pearson and Jones, 1965[34]), atmospheric pressure (Clements and Wilkening, 1974[35]), crustal radium deposits (Larson and Jeck, 1981[33]), and the strength of the radium source (Wilkening, 1974[36]). Radon levels of a few pCi/m^3 (picocuries per cubic meter) are typical over oceanic air, while concentrations of several tens of pCi/m^3 are found over land. An increase in radon concentration over ocean areas indicates the presence of an air mass with a recent overland history. Thus monitoring fluctuations in radon activity provides a technique for determining whether a given location is experiencing an intrusion of continental or maritime air.

The radon measurements were made by the Naval Research Laboratory at the micrometeorological tower facility which is located on the northwestern end of SNI about 20m from the high tide waterline (Blanc, 1978[1]). The instrumentation employed was developed by Larson (1973[37]) and utilizes a measurement technique that assumes equilibrium between radon and its daughter products (polonium 218, lead 214, bismuth 214). Radon levels are determined by collecting the daughter products on filter paper and measuring the beta activity with plastic scintillators optically coupled to photomultiplier tubes (Larson, 1973[37]; Larson and Bressan, 1978[38]). Although some questions have been raised concerning the assumption of equilibrium in radon daughter products (Shapiro et al., 1978[39]), it is well established that disequilibrium in maritime environments is unlikely except during rain when daughter products can be selectively removed (Larson, 1979a[40]; Gat, 1966[41]).

3. TRAJECTORY ANALYSIS TECHNIQUE

A computerized objective mesoscale analysis technique developed by Barnes (1973[42]) has been adapted by one of us (R. A. Helvey) to provide automatic determination of air parcel trajectories based on hourly surface wind observations at stations distributed over the region of interest. A trajectory is constructed from a series of vectors representing successive hourly displacements of a particular air parcel. Each of the individual displacements is obtained from wind components computed for the current position of the air parcel by use of the modified Barnes technique.

This technique interpolates wind observations from a number of stations to specified analysis points utilizing a Gaussian weight function of the form

$$W_i = \exp\left[-4R_i^2/D_s^2\right]$$

where W_i is the weight applied to the i th observation for the analysis point, R_i is the distance between the i th observation point and the analysis point, and D_s is a parameter that determines the response characteristics of the

---

[34]Pearson, J. E., and G. E. Jones, 1965: Emanation of radon 222 from soils and its use as a tracer. J. Geophys. Res., 70, 5279-5290. UNCLASSIFIED

[35]Clements, W. E., and M. H. Wilkening, 1974: Atmospheric pressure effects on 222 Rn transport across the earth-air interface. J. Geophys. Res., 79, 5025-5029. UNCLASSIFIED

[36]Wilkening, M. H., 1974: Radon-222 from the island of Hawaii: deep soils are more important than lava fields or volcanoes. Science, 183, 413-415. UNCLASSIFIED

[37]Larson, R. E., 1973: Measurements of radioactive aerosols using thin plastic scintillators. Nucl. Instrum. Methods., 108, 467-470. UNCLASSIFIED

[38]Larson, R. E., and D. J. Bressan, 1978: Automatic radon counter for continual operation. Rev. Sci. Instru., 49, 965-969. UNCLASSIFIED

[39]Shapiro, M. H., R. Kosowski, and D. A. Jones, 1978: Radon series disequilibrium in southern California coastal air. J. Geophys. Res., 83, 929-933. UNCLASSIFIED

[40]Larson, R. E., 1979a: Comment on 'Radon series disequilibrium in southern California coastal air' by M. H. Shapiro et al. J. Geophys. Res., 84, 751. UNCLASSIFIED

[41]Gat, J. R., G. Assaf, and A. Miko, 1966: Disequilibrium between the shortlived radon daughter products in the lower atmosphere resulting from their washout by rain. J. Geophys. Res., 71, 1525-1535. UNCLASSIFIED

[42]Barnes, S. L., 1973: Mesoscale objective map analysis using weighted time series observations. NOAA Technical Memorandum ERL NSSL-62, Mar. 1973. UNCLASSIFIED

weight function. Employing the exponential space weighting function allows all wind observations to objectively influence the values assigned at the analysis points. The analysis algorithm proceeds in two steps. First, a rough estimate of the analyzed wind is obtained using a relatively large value for D_S which effectively minimizes the contributions from small-scale irregularities in the observed data. Estimates are likewise obtained at the observation points themselves; these estimates are then subtracted from the original data to provide a correction field. In the next step the correction field is interpolated using a decreased D_S, which now permits smaller-scale features to influence the analysis. By reducing D_S in this manner, Barnes found that satisfactory pattern resolution could be achieved with considerably less computational effort than required by the widely-used Cressman (1959[43]) technique. For the station distribution in our study, an initial value of 60 nm for D_S, reduced to 15 nm for the second pass, appeared to yield the most satisfactory results. The final analysis value, P, for n observations is computed from

$$P = \sum_{i=1}^{n} W_i G_i \Big/ \sum_{i=1}^{n} W_i$$

where G_i is the weight the i th correction receives at the analysis point (Brandes, 1976[44]).

The analyses are carried out on a Hewlett-Packard 9845T Desktop Computer, which has a CRT (cathode-ray tube) and other features that make it particularly suited for interactive data entry, error detection and correction, and display of intermediate results. A number of steps necessarily precede the preparation of trajectories, including entering and storing station identifiers and locations and hourly wind data for the periods of interest. Hourly wind analyses can be generated to assist in checking for errors and in visualizing wind flow patterns; these are displayed on the CRT in the form of wind vectors plotted at grid points over the domain of analysis. Trajectories are plotted at hourly intervals within specified periods; they can be determined for durations up to 72 hours either forward or backward in time for specified points of origin or termination. Due to the scarce wind information available in our study and because of the meteorological uncertainties (mixing effects) inherent in following an air parcel, the trajectories discussed in this report are for 24-hour duration. Since the objective was to determine possible effects of previous history of air parcel characteristics, they were obtained backward in time from a given termination point (SNI).

Analyses were performed for a 330 x 260 nm region centered near SNI. Hourly surface wind directions and speeds for 12 southern California coastal and island weather stations were used. In addition, winds were estimated from surface weather charts for three points (P1, P2, P3) over the open ocean. The trajectory computations are terminated if the path passes outside the map boundaries. Topographical and air mass mixing effects are ignored, thus only horizontally advected, near-surface, air motions are considered. In the future, low-level cloud motion vectors derived from successive geostationary satellite imagery will also be incorporated to obtain estimates of winds over data-sparse oceanic areas. The locations of all 15 sites are listed in Table 1.

4. COMPARISON OF AIR TRAJECTORIES AND RADON LEVELS

Figure 3a illustrates, for the five EOMET/OSP measurement periods, a total of 273 24-hour trajectories terminating at SNI during periods when radon measurements were available. Most of the trajectories originate from locations north of SNI and a conspicuous trajectory void exists to the southeast. Radon amounts were observed to vary by more than two orders of magnitude; the largest radon level recorded was 126.1 pCi/m^3 and the smallest was 0.8 pCi/m^3. The large variability observed in air parcel history and radon activity (figure 3a), which results primarily from the superimposition of different air mass regimes, can be resolved into trajectory paths that correspond to distinct radon concentration categories. Samson (1980[45]) has successfully used a similar approach to study air trajectories and sulfate aerosols. In our investigation we have found three radon concentration categories (low: <10

[43] Cressman, G. P., 1959: An operational objective analysis system. Mon. Wea. Rev., 87, 367-374. UNCLASSIFIED

[44] Brandes, E. A., 1976: Hourly surface weather maps and analyzed fields of meteorological variables. NOAA Technical Memorandum ERL NSSL-80, Dec. 1976. UNCLASSIFIED

[45] Samson, P. J., 1980: Trajectory analysis of summertime sulfate concentrations in the Northeastern United States. J. Appl. Meteor., 19, 1382-1394. UNCLASSIFIED

Table 1. Station Locations Used in Trajectory Computations.

Identifier	Location	Longitude (West)	Latitude (North)
SMX	Santa Maria	120.417°	34.933°
SBA	Santa Barbara	119.833°	34.433°
LAX	Los Angeles	118.383°	33.933°
SNA	Santa Ana	117.867°	33.667°
SAN	San Diego	117.167°	32.733°
VBG	Vandenberg Air Force Base	120.567°	34.733°
NTD	Point Mugu	119.117°	34 177°
NUC	San Clemente Island	118.583°	33.017°
NFG	Oceanside	117.367°	33.300°
SM4	San Miguel Island	120.363°	34.033°
SZ1	Santa Cruz Island	119.634°	33.995°
SN5	San Nicolas Island (Site A)	119.575°	33.277°
P_1	Open Ocean	122.000°	35.000°
P_2	Open Ocean	121.000°	33.000°
P_3	Open Ocean	119.000°	32.000°

pCi/m^3; medium: $\geq$10, $<$30 pCi/m^3; high: $\geq$30 pCi/m^3) useful in distinguishing between the air flow patterns depicted in figure 3a. Figures 3b, 3c and 3d show the trajectory paths corresponding to the low, medium, and high radon concentration categories respectively. The lowest radon levels (figure 3b) occurred when the air traversed a northwesterly to westerly oceanic path before ending at SNI. In general, the highest radon concentrations (figure 3d) were associated with air parcels that either passed over land or through the southern California bight. The northwesterly trajectories are observed to involve brisk regular wind speeds while other directions primarily involve upstream stagnation. Trajectories corresponding to the medium radon category (figure 3c) consist of paths that are similar to those found in both the high and low radon concentration groups. This is suggestive of a transition mode if we think of successive changes in radon reflecting similar changes in the air trajectories.

Table 2 summarizes the trajectory/radon sample size according to radon category for the individual measurement periods and figures 4, 5, and 6 illustrate the trajectory paths for each period and radon category. In figure 5a, relatively high radon concentrations were observed for both the northwest (parallel to the coast line) and southwest (towards the open sea) trajectories, suggesting earlier overland travel or horizontal/vertical mixing with continental air. The two overwater trajectories passing near P1 in figure 5d are also associated with high radon levels; however, while these trajectory paths may at first appear similar to those corresponding to the low radon category in figure 4, they are, in fact, distinctly different in that they turn into the southern California bight just to the north of San Miguel Island. It is noteworthy that the two northwesterly trajectories observed in figure 6d, during the transition regime, correspond to radon levels of 14.1 and 14.7 pCi/m^3 while the other two trajectories, which traverse the bight region, correspond to radon values of 25.3 and 27 pCi/m^3. The two westerly trajectories shown in figure 6e ended at SNI simultaneous with radon measurements of 10.5 and 12.5 pCi/m^3.

Table 2. Trajectory/Radon Sample Size for Radon Concentration Categories During Each of the Five Experiments.

Measurement Period	Radon Concentration (pCi/m^3)		
	$<$10	$\geq$10, $<$30	$\geq$30
780508-780522	11	44	24
781106-781117	1	6	9
790425-790511	54	15	1
800113-800125	16	4	41
800721-800731	45	2	0
TOTAL SAMPLE SIZE =	127 +	71 +	75 = 273

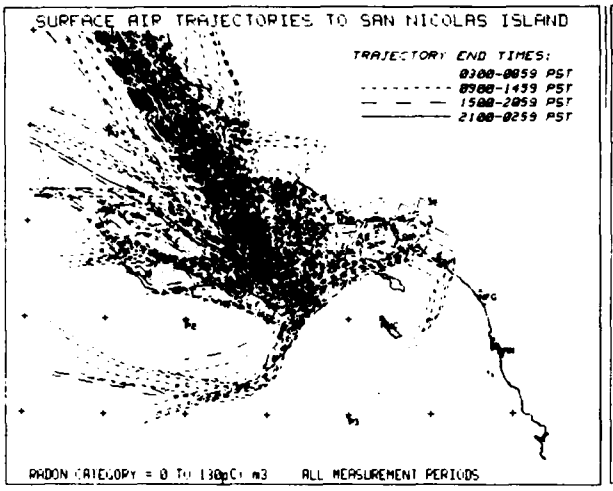

Figure 3(a).

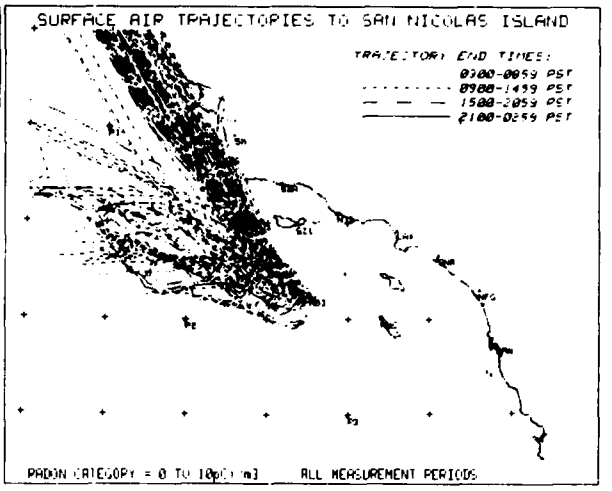

Figure 3(b).

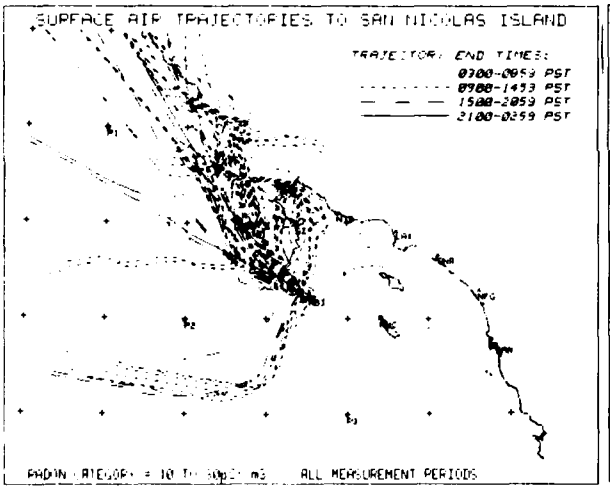

Figure 3(c).

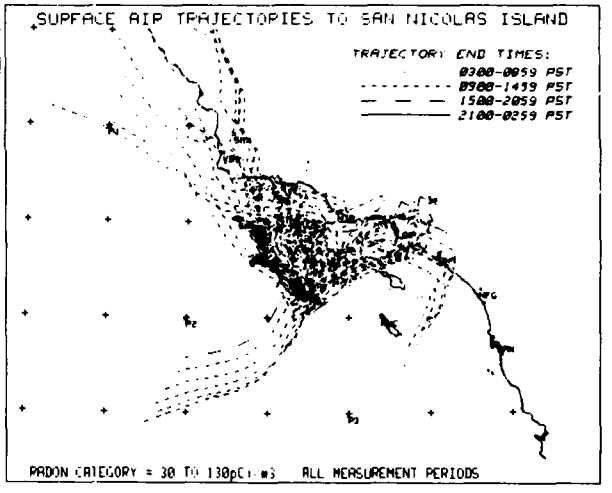

Figure 3(d).

Figure 3. Air trajectories ending at SNI for all measurement periods are illustrated with their resolution into the low (<10 pCi/m^3), medium (≥10, <30 pCi/m^3), and high (≥30 pCi/m^3) radon categories. Note the trajectory paths "filling in" the southern California bight area as the radon concentration category increases.

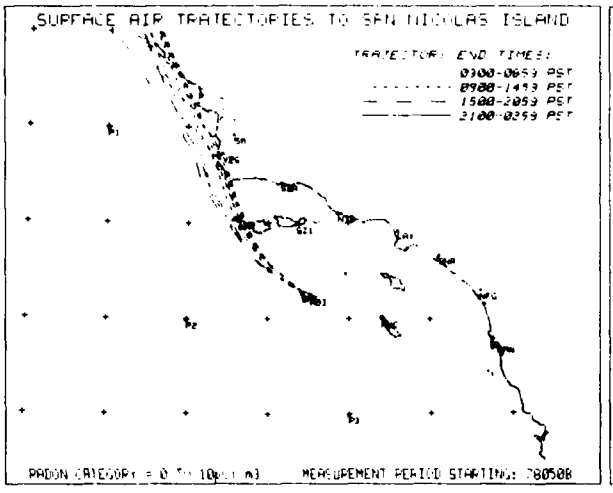

Figure 4(a).

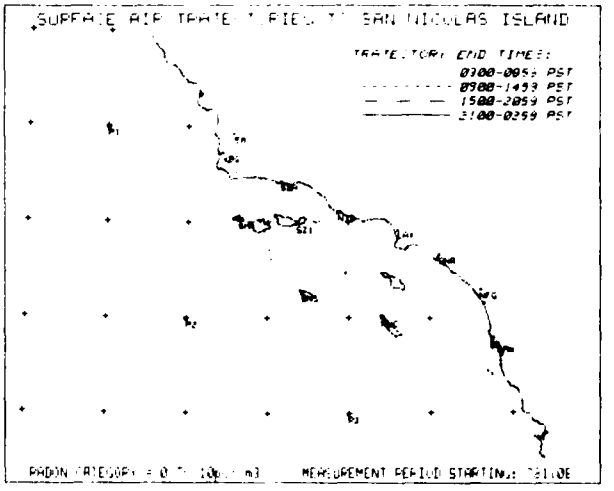

(Figure 4(b).

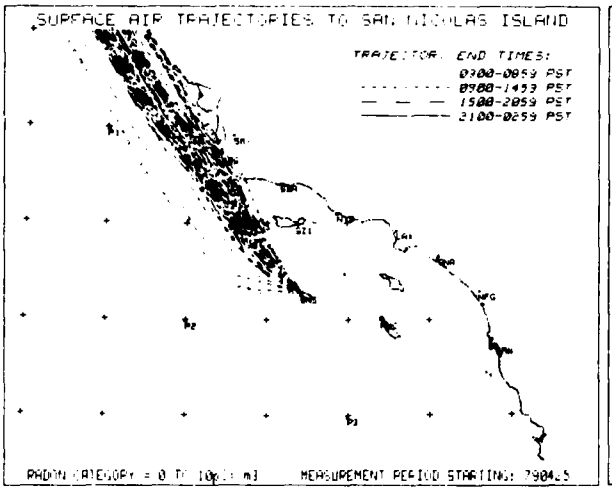

Figure 4(c).

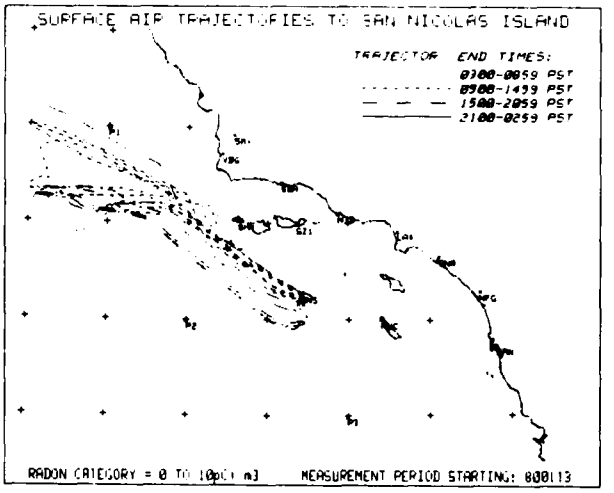

(Figure 4(d).

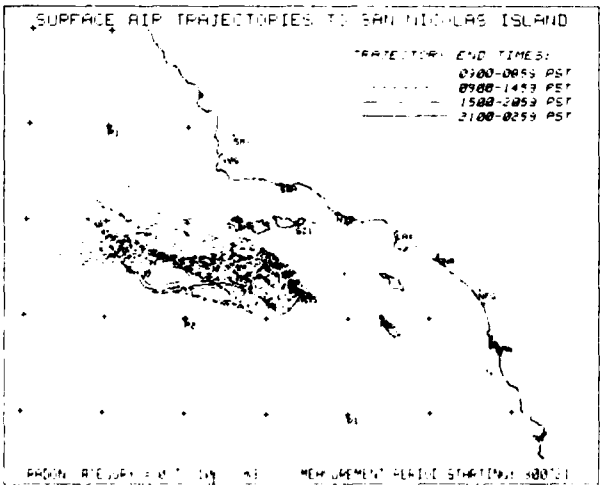

Figure 4(e).

Figure 4. Air trajectories terminating at SNI during each measurement experiment are illustrated for the low (<10 pCi/m^3) radon category. In general, low radon levels measured at SNI are associated with a mostly overwater northwesterly to westerly trajectory pattern.

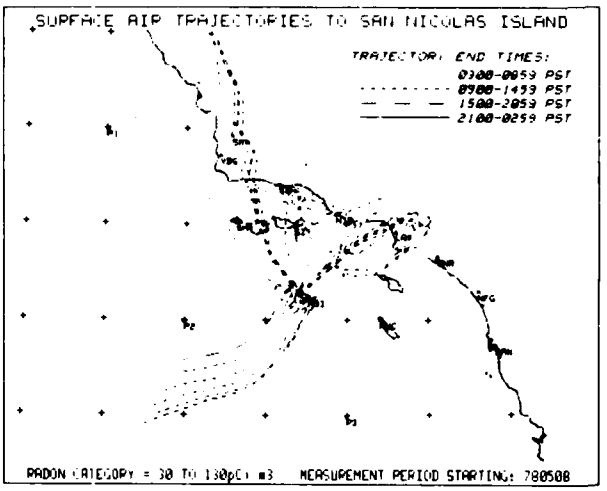

Figure 5(a).

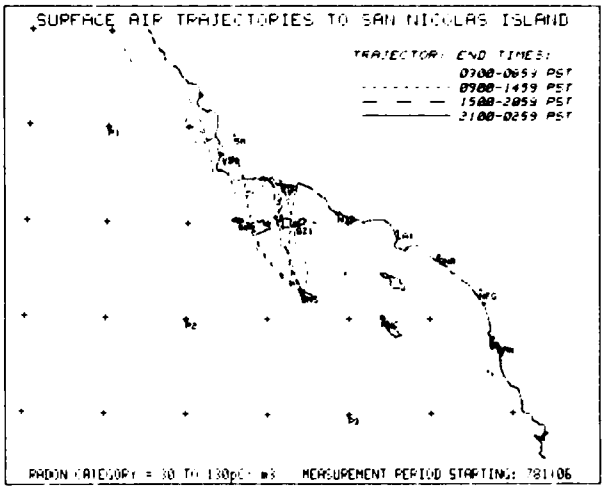

Figure 5(b).

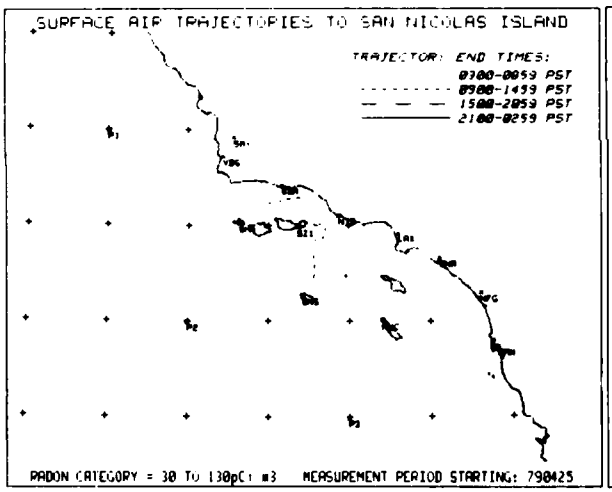

Figure 5(c).

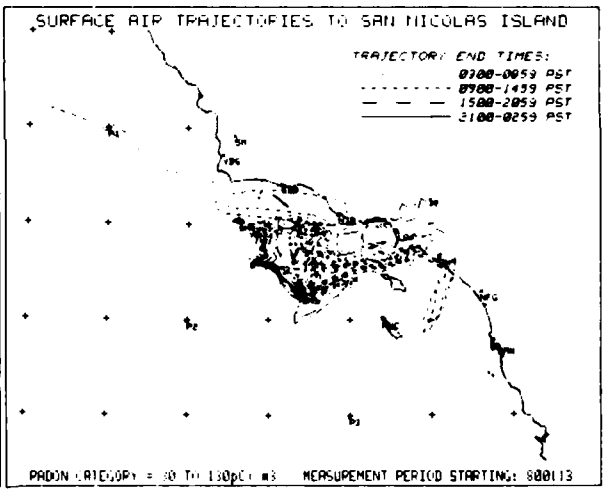

Figure 5(d).

Figure 5. Air trajectories ending at SNI during each measurement experiment are illustrated for the high (>30 pCi/m^3) radon category. High radon levels were not observed during the last experiment (July 1980). In general, high radon levels measured at SNI are associated with air trajectories that have a history over land or in the southern California bight.

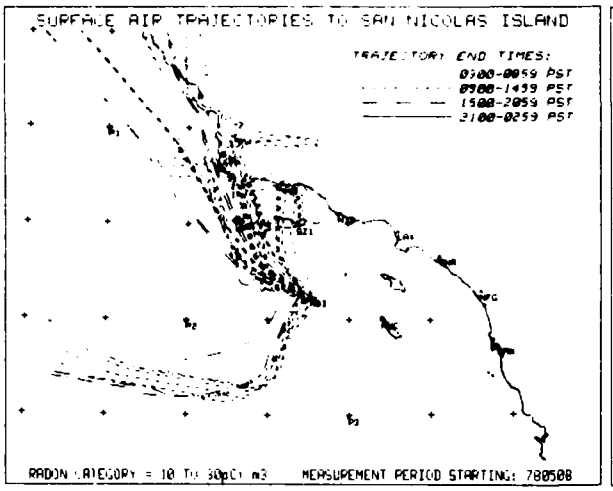

Figure 6(a).

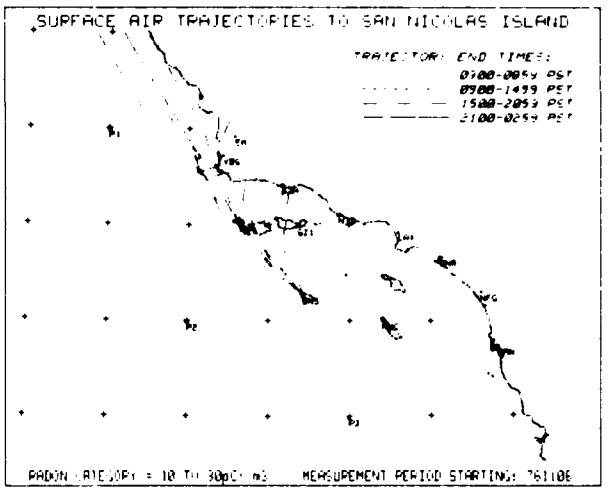

Figure 6(b).

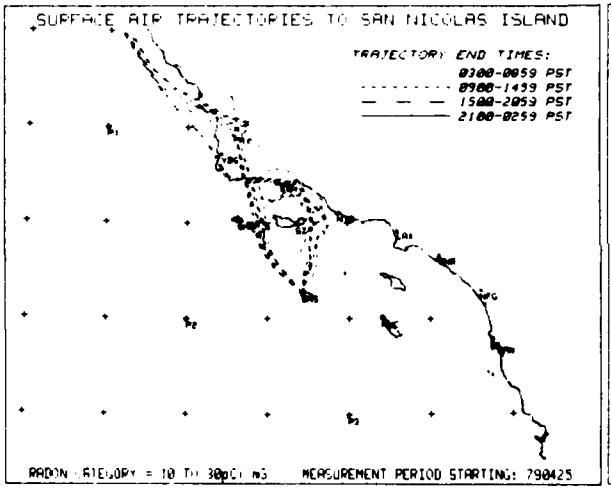

Figure 6(c).

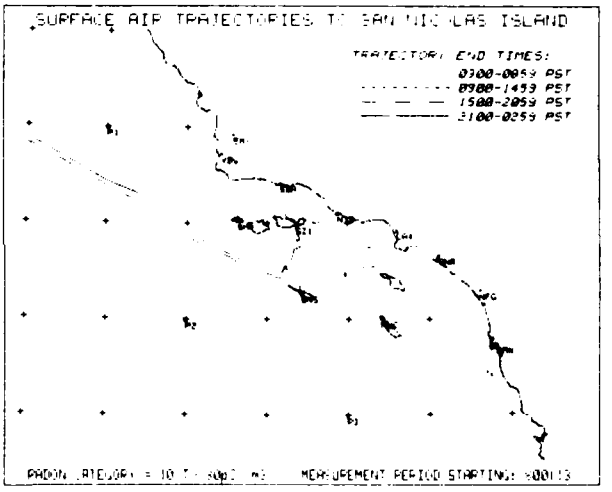

Figure 6(d).

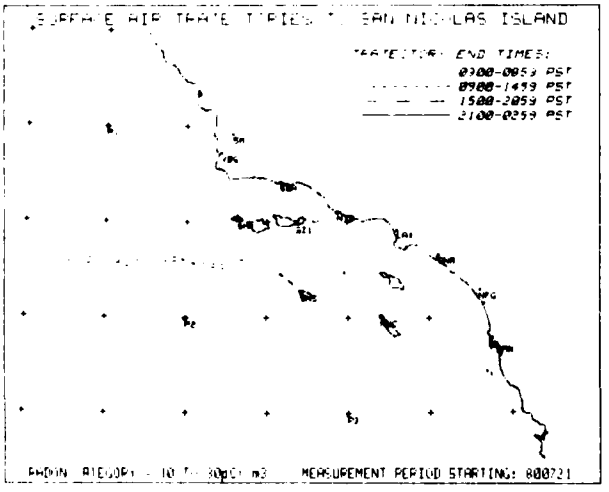

Figure 6(e).

Figure 6. Air trajectories terminating at SNI during each measurement experiment are illustrated for the medium (>10, <30) radon category. These maps exhibit trajectory paths that are similar to those found in both the low and high radon concentration categories and are suggestive of a transition mode.

5. SYNOPTIC CONDITIONS AND RADON LEVELS

The most striking difference in trajectory paths occurs between the low (figure 3b) and high radon (figure 3d) concentration categories. Some of the essential and representative meteorological features responsible for this bifurcation will now be discussed. First we attempt an explanation of the two "anomalous" cases, i.e., the events where relatively high radon levels were associated with overwater trajectories, by recourse to the meteorological conditions that produced them.

a. May 1978

In all of the periods studied, good agreement was observed between trajectory paths and radon measurements except during the May 1978 experiment when high radon levels were recorded for two episodes of overwater trajectories. The first episode, which consists of the southwesterly trajectory paths exhibited in figure 5a, occurred on May 14, 1978 when a well defined "Catalina eddy," illustrated in figure 7, became established in the southern California bight in the wake of a "Santa Ana" (offshore flow) condition. A number of factors could have contributed to the measurement of high radon levels coincident with the oceanic trajectory paths. Four possible explanations follow: (1) radon may have been advected from land and/or from the post "Santa Ana" air by the eddy circulation while limited wind information over the ocean could have resulted in inaccurate trajectories; (2) above background radon exhalation from southwest SNI could have been transported to the measurement site by the observed trajectories; (3) if the trajectories were extended backwards far enough they may reveal an overland history that could account for all or part of the high radon values (the trajectories terminate near the southwest map boundary when extended out to 48 hours); (4) the observed surface air trajectories may be accurate but not completely representative of the air mass history due to horizontal and vertical mixing effects that have been neglected by our treatment. In any event it appears likely that the cyclonic (counterclockwise) eddy circulation transported radon from land and/or from post "Santa Ana" air and through the bight.

The second episode during which high radon activity was associated with overwater trajectories occurred about one week later and is distinguished by the two northwesterly paths in figure 5a. The pacific high pressure system west of Washington, shown in figure 8a, apparently circulated air along an overland coast route where high radon levels could be accumulated, then turned offshore tracing out the northwesterly path illustrated in figure 5a.

b. November 1978

The trajectory paths for the November 1978 measurement period (figures 4b, 5b, and 6b) are somewhat similar to each other and were associated with high pressure off the coast extending inland over northern California and Oregon (figure 8b). Offshore pressure gradients, and therefore higher radon concentrations, were established due to inland ridging to the north in the wake of transient short wave troughs. The air traversing the northern coast still retained some continental (higher radon) characteristics after its short over-water transit to SNI.

c. April/May 1979

Figure 5c shows only a single trajectory for the high radon concentration category during the April/May 1979 experiment. The synoptic features producing this pattern are illustrated in figure 8c and are similar to those discussed in section 5b. A weak offshore pressure gradient developed over southern California as the semipermanent Pacific high was distorted by the short wave passage over the ridge.

Most of this period was dominated by the strong northwesterly trajectory pattern shown in figure 4c. These trajectories were supported by an intense high pressure system located over the Pacific. Figure 8d shows an example of the synoptic conditions when radon levels at SNI were 2 pCi/m^3 and the trajectories from the regime in figure 4c. The lowest radon levels for all five measurement periods were observed during this episode.

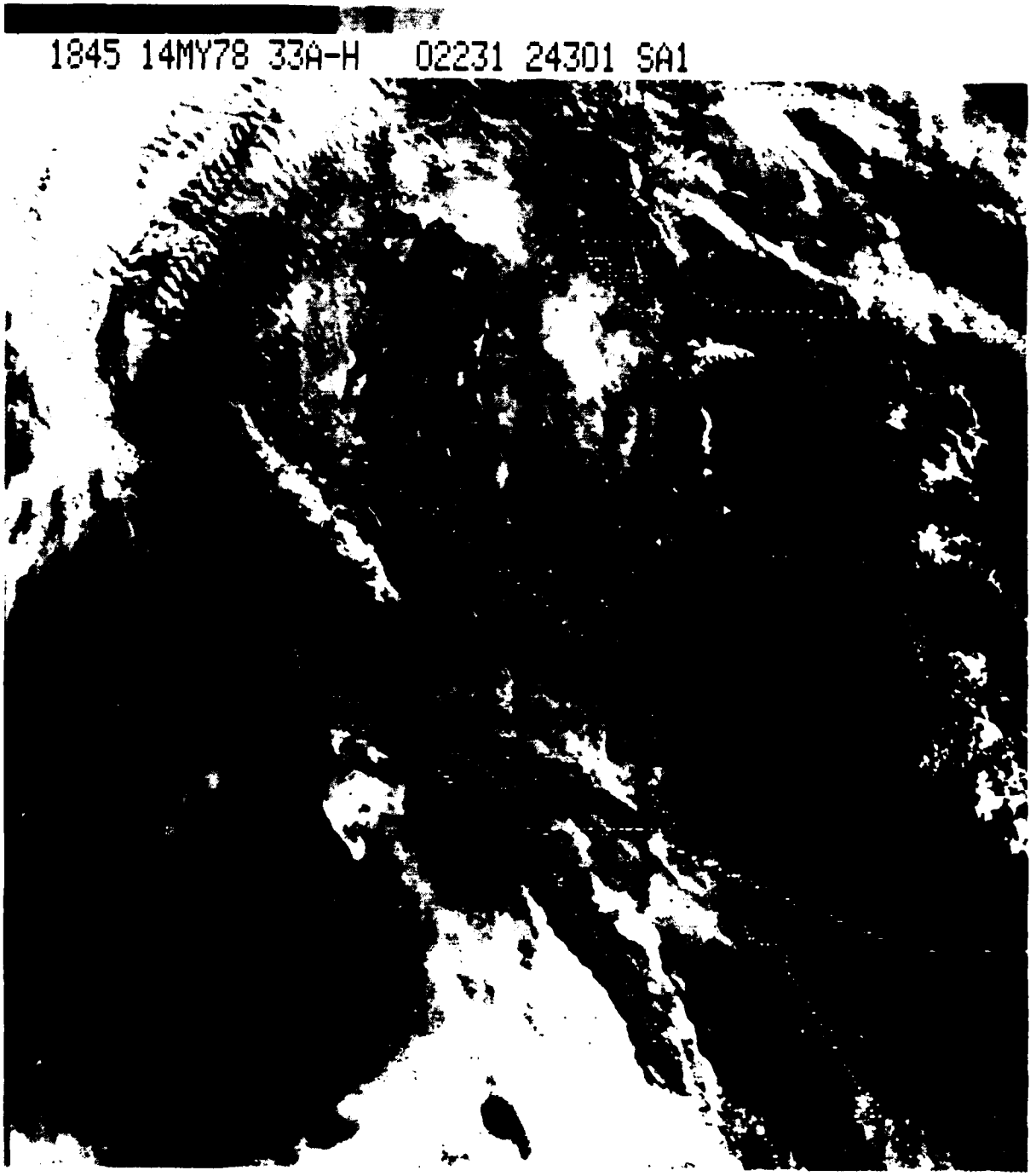

Figure 7. GOES Satellite Imagery at 1845Z (1045 PST) – 14 May 1978. Catalina Eddy Engulfs Southern California Bight in Marine Stratus.

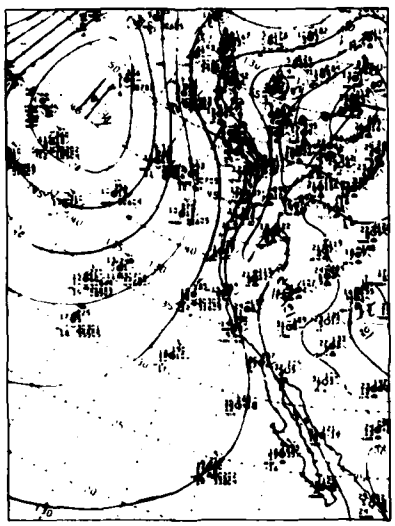

Figure 8A. 21 May 78 (1800 Z)

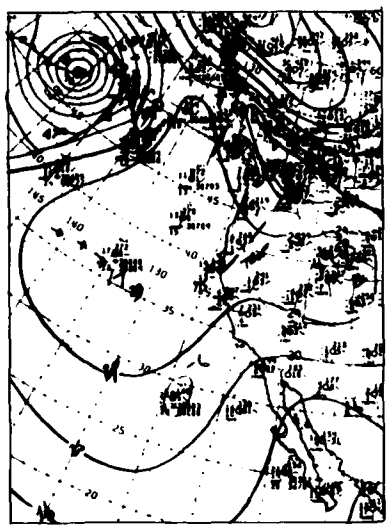

Figure 8B. 17 Nov 78 (1200 Z)

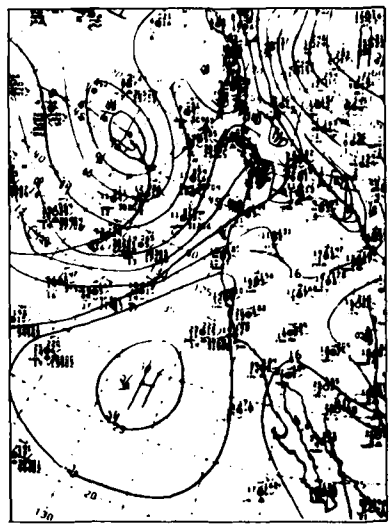

Figure 8C. 04 May 79 (1800 Z)

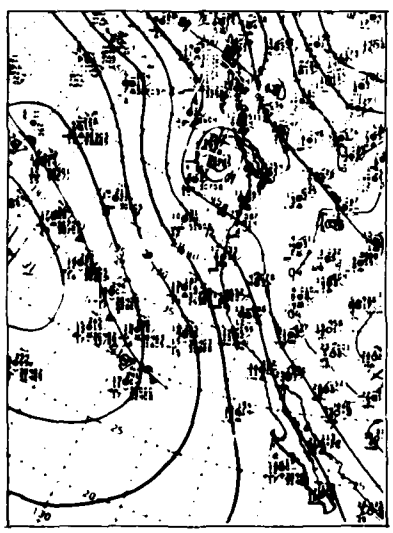

Figure 8D. 07 May 79 (1800 Z)

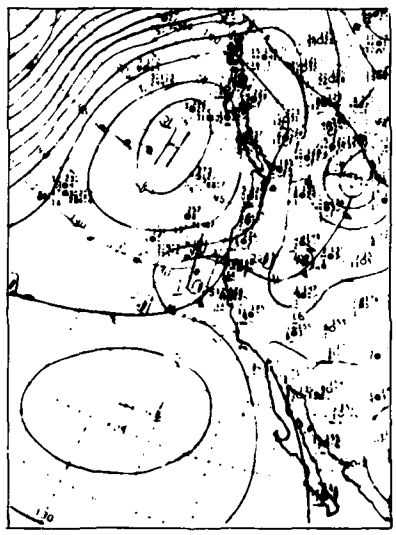

Figure 8E. 17 Jan 80 (1200 Z)

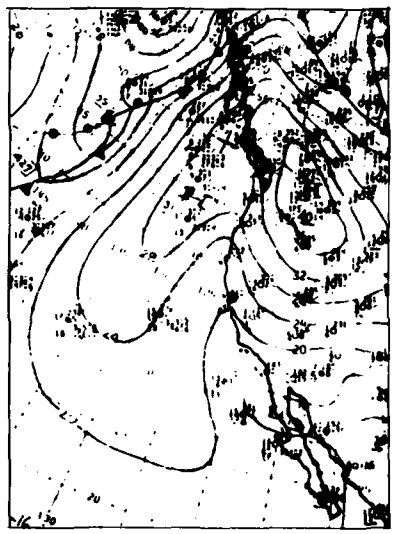

Figure 8F. 22 Jan 80 (1200 Z)

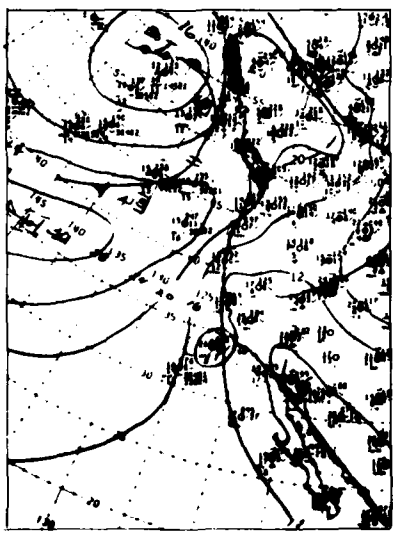

Figure 8G. 24 Jul 80 (1200 Z)

Figure 8. Pacific Surface Weather Analysis Charts for Selected Periods During the EOMET/OSP Experiments (1978-1980) on SNI.

d. January 1980

Figures 4d and 5d illustrate the greatest dichotomy in trajectory paths for an individual measurement period. The low radon trajectories in figure 4d were associated with the movement of a frontal system across the northern fringe of the Pacific High as shown in figure 8e. As the front moved southeastward and passed through the southern California area, onshore pressure gradients with northwesterly trajectories and low radon levels were maintained.

The high radon trajectories in figure 5d resulted, for the most part, from a strong, high pressure, build up over the Great Basin that established weak offshore pressure gradients over southern California. This weather system is outlined in figure 8f and was responsible for relatively stagnant air circulation in the bight.

e. July 1980

Only low radon measurements with westerly trajectory paths, shown in figure 4e, were observed during the July 1980 experiment. The air mass conditions for this episode were characterized by air arriving from the periphery of the Pacific High blowing towards the thermal trough over inland southern California as illustrated in figure 8g. Weak onshore pressure gradients, sustained by the combination of the Pacific High and thermal trough, produced the light westerly winds and low radon levels measured at SNI.

6. RADON VERSUS INVERSION ALTITUDE

Rawinsonde data from SNI was used to construct time series plots of potential temperature for altitudes from the surface up to 6000 ft. The base of the marine inversion layer was then approximated as the height at which isentropic packing was observed on the time series graphs. Figure 9a shows the scatter diagram obtained for radon concentration as a function of inversion altitude for all measurement periods when data was available. Evidently, a general trend for higher radon levels is indicated when the height of the inversion base is low, and only low radon values are observed for the largest inversion altitudes. Furthermore, figure 9a also indicates a lack of dependence between radon activity and inversion height when radon levels are less than 10 pCi/m^3. The data stratum in low radon activity and the general clustering of data in figure 9a are suggestive of an interdependence between radon and inversion altitude and warrants further attention.

Figures 9b and 9c illustrate the trajectory paths when the inversion altitude is above 750 ft. and radon levels are <10 pCi/m^3 and >10 pCi/m^3 respectively. Figures 9d and 9e show the trajectories for the same radon categories but for inversion altitudes below 750 ft. From figures 9b and 9c, we generally find high inversion (>750 ft) conditions corresponding to swift northwesterly trajectories with low (figure 9b) and high (figure 9c) radon levels depending upon the trajectory route. In contrast, low inversion conditions are mostly associated with high radon concentrations and upstream stagnation in the bight (figure 9e); a few cases of low radon overwater paths also occur (figure 9d). Since the distribution of atmospheric radon generally decreases exponentially with altitude (Jacobi and Andre, 1963[46]; Larson and Hoppel, 1973[47]), the higher inversion altitudes may, in some cases, allow radon-rich air near the land surface to mix with radon-poor air at higher elevations. Low inversion conditions, by comparison, favor the suppression of deep vertical mixing and provide, in the presence of weak offshore pressure gradients, ideal conditions for high radon levels and the relatively stagnant trajectories observed in the southern California bight (figures 5a, 5c, 5d). In order to completely account for mixing processes, 3-dimensional air motions over longer time scales should be considered.

---

[46] Jacobi, W., and K. Andre, 1963: The vertical distribution of Radon 222, Radon 220 and their decay products in the atmosphere. J. Geophys. Res., 68, 3799-3814. UNCLASSIFIED

[47] Larson, R. E., and W. A. Hoppel, 1973: Radon 222 measurements below 4 Km as related to atmospheric convection. Pageoph., 105, 900-906. UNCLASSIFIED

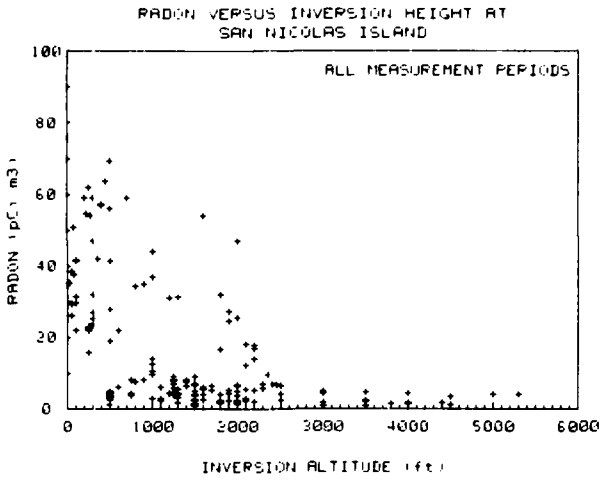

Figure 9(a).

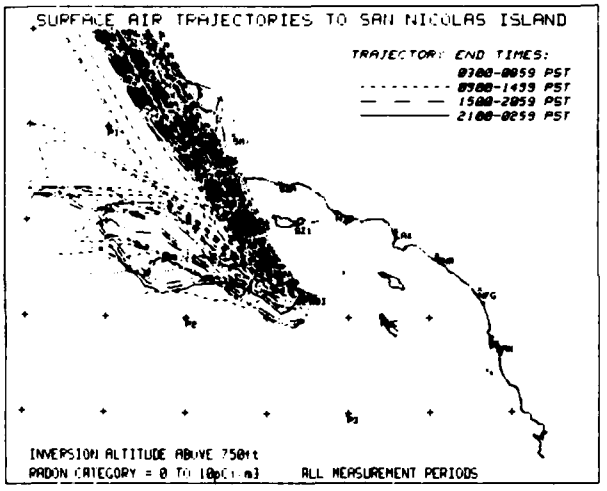

Figure 9(b).

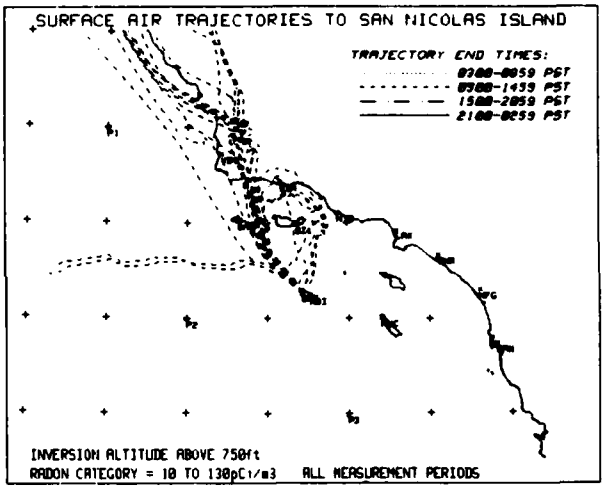

Figure 9(c).

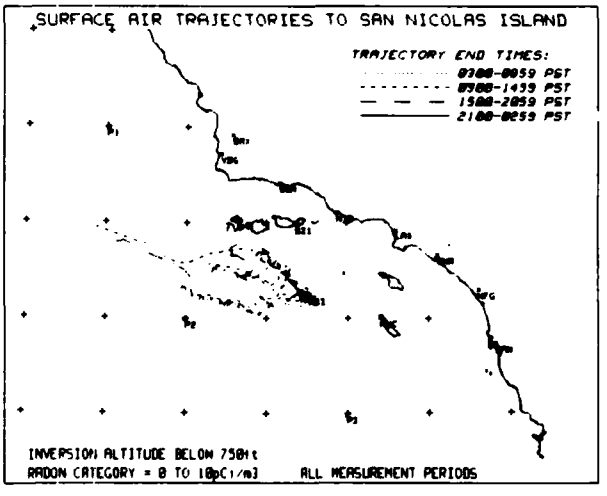

Figure 9(d).

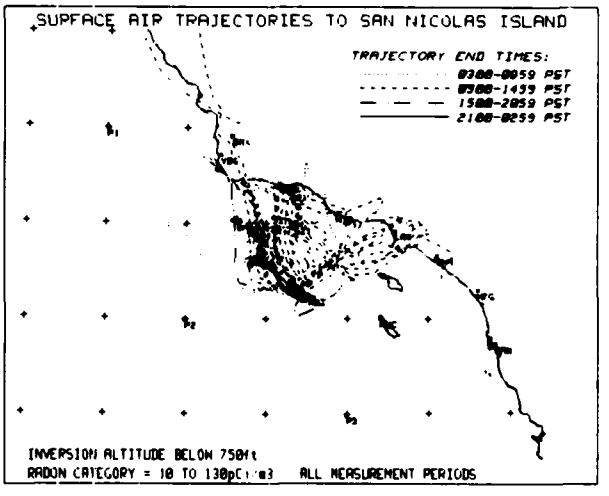

Figure 9(e).

Figure 9. Scatter diagram shows relationship between radon concentration and the approximate altitude of the base of the marine inversion layer for available data during the five experiments. Figures 9(b)–9(e) illustrate trajectory paths isolated according to radon category and inversion altitude.

7. RADON VERSUS AIR PARCEL SPEED

Some of the 24-hour trajectories that are coincident with low radon activity terminate off the map boundaries (figure 9b), indicating high wind speeds, while other paths that are associated with high radon concentrations, reveal much shorter histories (figure 9e) and therefore, lower wind speeds. To study this relationship further, we computed the average air parcel speed along trajectories for up to 48 hours. Plots of radon concentration versus average wind speed for trajectories of various durations (3, 6, 9 . . . 48 hrs.) show a tendency for high radon levels to occur at low wind speeds and low radon levels to occur at high wind speeds. Figure 10a shows the results for 12-hour trajectories during all measurement episodes and figure 10b illustrates the contribution of the April/May 1979 period to figure 10a. Each measurement period exhibited the same trend except for the July 1980 experiment (figures 4e, 6e) when low radon levels were observed with light westerly winds.

8. PSEUDO MEAN RADON DISTRIBUTION

Figure 11 was produced in an effort to parameterize some of the relationships that we have observed between air trajectories and radon measurements at SNI. This map illustrates the distribution of average radon levels for 12-hour trajectories passing over the regions where the values are indicated. For example, figure 11 shows us that the average radon concentration measured at SNI for trajectories that pass over Santa Catalina Island (see figure 1) before arriving at SNI is approximately 50 pCi/m^3. As observed earlier, but now more quantitatively, we find the highest average radon levels measured at SNI occur for air parcels passing over land or through the bight; whereas the lowest levels occur for air that passes over water from the west and northwest of SNI.

Because any air parcel traced sufficiently backward in time will ultimately traverse the open ocean, the technique discussed here should be limited to short air parcel histories. The choice of the 12-hour trajectories was a compromise based upon this constraint. Trajectories of 24- and 48-hour durations reveal the same trend in average radon distribution, but with different magnitudes. In the future we will attempt to quantify these results further by deriving effective radon emission rates in lieu of the average radon values in figure 11, based on the distribution of trajectory paths and the single station radon measurements.

9. CONCLUSIONS

Despite the simplicity of the trajectory technique used here, which neglects topographical, vertical/horizontal mixing, and dynamical effects, and considering the uncertainties involved in reconstructing air parcel history from the scarce wind information available, the trajectories are in general agreement with the radon measurements. The bulk of the radon fluctuations are explained by trajectory, although inverse correlations between radon and inversion height, and radon and wind speed were also observed. Because sufficient wind data for constructing air trajectories is not available in many areas, radon is a valuable diagnostic tool that can be used in realtime operational situations or in subsequent analyses. However, if a predictive capability is desired for assessment of electro-optical conditions, air mass trajectories constructed from forecast wind fields must be employed. We believe that some effort should be devoted to developing an air mass index, based upon trajectory, which can be used in aerosol models for predicting electro-optical extinction in the same fashion that radon is used as a realtime air mass parameter (Gathman, 1982[19]). Our results suggest the use of marine aerosol models for predicting extinction coefficients when radon levels are less than 10 pCi/m^3; for radon levels $\geq$30 pCi/m^3, continental aerosol models would be appropriate. Caution should be exercised here since these results apply only to SNI and should not be used for other locations, where geological features and crustal radium deposits may differ substantially (Larson et al., 1982[48]), unless confirmed by some trajectory technique. Similar trajectory/radon relationships can be determined for other areas of interest and, in this fashion, radon levels can be "calibrated" to the local marine/continental conditions. To test our findings and to more fully determine the impact air mass effects have on aerosol properties, future investigations should explore the feasibility of using radon and air trajectories to characterize aerosol size distributions.

---

[48]Larson, R. E., D. J. Bressan, and P. E. Wilkniss, 1982: Atmospheric measurements by the Atmospheric Physics and Chemical Oceanography Branches. NRL report in press, 1982. UNCLASSIFIED

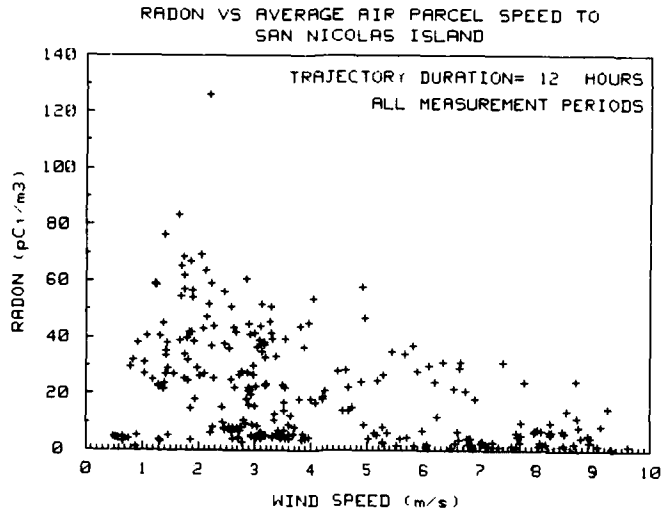

Figure 10(a).

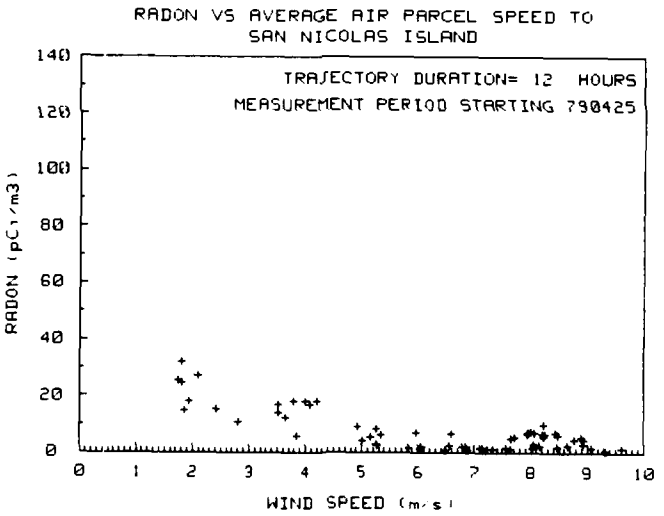

Figure 10(b).

Figure 10. Radon concentration plotted against average wind speed for 12-hour trajectories during all measurement periods (figure 10a) and during the April/May 1979 experiment (figure 10b).

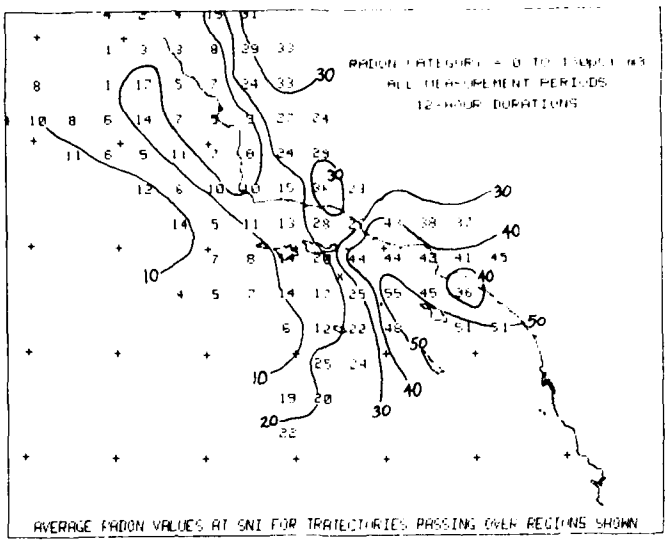

Figure 11. Plotted numbers and isopleths indicate average radon concentrations (measured at SNI) for 12-hour trajectories (ending at SNI) passing over the indicated areas.

REFERENCES

1. Blanc, T. V., 1978: Micrometeorological data for the Cooperative Experiment for West Coast Oceanography and Meteorology (CEWCOM-78) at San Nicolas Island, California Vol. I and II. NRL Memorandum Report 3871, Aug. 1978. UNCLASSIFIED

2. Blanc, T. V., 1979: Micrometeorological data report for the November 1978 Electro-Optics Meteorology (EOMET) experiment at San Nicolas Island, California. NRL Memorandum Report 4056, Aug. 1979. UNCLASSIFIED

3. Blanc, T. V., 1981: Report and analysis of the May 1979 Marine surface layer micrometeorological experiment at San Nicolas Island, California. NRL Report 8363, Dec. 1981. UNCLASSIFIED

4. Blanc, T. V., 1982: The data base for the May 1979 marine surface layer micrometeorological experiment at San Nicolas Island, California. NRL Report 4713, May 1982. UNCLASSIFIED

5. Matthews, G. B., B. E. Williams, A. Akkerman, J. Rosenthal, and R. de Violini, 1978: Atmospheric transmission and supporting meteorology in the marine environment at San Nicolas Island–semiannual report. PACMISTESTCEN Technical Report TP-79-19, Dec. 1978. UNCLASSIFIED

6. Jeck, R. K., 1979: Aerosol particle size measurements at San Nicolas Island during CEWCOM-78. NRL Memorandum Report 3931, Mar. 1979. UNCLASSIFIED

7. Rosenthal, J., T. E. Battalino, V. R. Noonkester, and H. Hendon, 1979: Marine/continental history of aerosols at San Nicolas Island during CEWCOM-78 and OSP III. PACMISTESTCEN Technical Publication TP-79-33, Apr. 1979. UNCLASSIFIED

8. Clark. R., T. E. Battalino, R. Helvey, and J. Rosenthal, 1981a: Atmospheric conditions and airmass history at San Nicolas Island during the November 1978 EOMET/OSP experiment. PACMISTESTCEN Technical Publication TP-81-30, Dec. 1981. UNCLASSIFIED

9. Clark, R., T. E. Battalino, and R. Helvey, 1981b: Atmospheric conditions and airmass history at San Nicolas Island during the 30 April-11 May 1979 EOMET/OSP experiment. PACMISTESTCEN Technical Publication TP-81-33, Dec. 1981. UNCLASSIFIED

10. Clark, R., T. E. Battalino, and R. Helvey, 1982a: Atmospheric conditions and airmass history at San Nicolas Island during the 14-25 January 1980 EOMET/OSP experiment. PACMISTESTCEN Technical Publication TP-82-21, May 1982. UNCLASSIFIED

11. Clark, R., T. E. Battalino, and R. Helvey, 1982b: Atmospheric conditions and airmass history at San Nicolas Island during the 22-31 July 1980 EOMET/OSP experiment. PACMISTESTCEN Technical Publication TP-82-22, May 1982. UNCLASSIFIED

12. Barnhart, E. A., and J. L. Streete, 1970. A method for predicting atmospheric aerosol scattering coefficients in the infrared. Applied Optics, 9, 1337-1344. UNCLASSIFIED

13. Wells, W. C., G. Gal, and M. W. Munn, 1977: Aerosol distributions in maritime air and predicted scattering coefficients in the infrared. Appl. Opt., 16, 654-659. UNCLASSIFIED

14. Katz, B. S., K. Hepfer, and N. E. MacMeekin, 1979: Electro-optics meteorological sensitivity study. NSWC TR-79-67, Apr. 1979. UNCLASSIFIED

15. Richter, J. H., and H. G. Hughes, 1981: Electro-optical atmospheric transmission effort in the marine environment. NOSC Technical Report 696, May 1981. UNCLASSIFIED

16. Hughes, H. G., and J. H. Richter, 1979: Extinction coefficients calculated from aerosol size distributions measured in a marine environment. Proceedings of the Society of Photo-Optical Instrumentation Engineers, San Diego, CA., Aug. 29-30, 1979. UNCLASSIFIED

17. Noonkester, V. R., 1980: Offshore aerosol spectra and humidity relations near southern California. Second Conference on Coastal Meteorology, Los Angeles, CA., Jan. 30-Feb. 1, 1980. UNCLASSIFIED

18. Hughes, H. G., 1980: Aerosol extinction coefficient variations with altitude at 3.75 um in a coastal marine environment. J. Appl. Meteor., 19, 803-808. UNCLASSIFIED

19. Gathman, S. G., 1982: Navy aerosol model. Paper presented at the Annual Review Conference on Atmospheric Transmission Models, AFGL, Hanscom AFB, Mass., May 18-19, 1982. UNCLASSIFIED

20. Wilkening, M. H. and W. E. Clements, 1975: Radon 222 from the ocean surface. J. Geophs. Res., 80, 3828-3830. UNCLASSIFIED

21. Larson, R. E., D. J. Bressan, K. W. Marlow, T. A. Wojciechowski, and J. L. Heffter, 1979c: A comparison of concentrations of fission products, Radon 222, and cloud condensation nuclei over the North Atlantic. Pageoph., 117, 874-882. UNCLASSIFIED

22. Fontan, J., D. Blanc, and A. Bouville, 1963: Meteorological conditions dependance of radon concentrations in air above the Atlantic. Nature, 197, 583-584. UNCLASSIFIED

23. Vilenskii, V. D., G. V. Dmitrieva, and Yu. Kirasnopovtrev, 1967: Natural and artificial radioactivity of the atmosphere over the ocean and its relation to meteorological factors. U.S. Atomic Energy Commission Report AEC-TR-6711. UNCLASSIFIED

24. Rama, K., 1970: Using natural radon for delineating monsoon circulation. J. Geophys. Res., 75, 2227-2229. UNCLASSIFIED

25. Prospero, J. M., and T. N. Carlson, 1970: Radon-222 in the North Atlantic Trade Winds: its relationship to dust transport from Africa., Science, 167, 974-977. UNCLASSIFIED

26. Wilkniss, P. E., R. E. Larson, D. J. Bressan, and J. Steranka, 1974: Atmospheric and continental dust near the antarctic and their correlation with air mass trajectories computed from Nimbus 5 satellite photographs. J. Appl. Meteor., 13, 512-515. UNCLASSIFIED

27. Moore, H. E., S. E. Poet, E. A. Martell, and M. H. Wilkening, 1974: Origin of 222 Rn and its long-lived daughters in air over Hawaii. J. Geophys. Res., 79, 5019-5024. UNCLASSIFIED

28. Subramanian, S. K., C. Rangarajan, S. Gopalakrishnan, and C. D. Eapen, 1977: Radon daughter's radioactivity levels over the Arabian Sea as indicators of air mass mixing. J. Appl. Meteor., 16, 487-492. UNCLASSIFIED

29. Larson, R. E., 1978: Radon 222 measurements during marine fog events off Nova Scotia. J. Geophys. Res., 83, 415-418. UNCLASSIFIED

30. Larson, R. E., 1979b:Atmospheric 222 Rn measurements at San Nicolas Island. NRL Technical Memorandum Report 4099, Nov. 1979. UNCLASSIFIED

31. Larson, R. E., W. Kasemir, and D. J. Bressan, 1979: Measurements of atmospheric 222 Rn at San Nicolas Island and over nearby California coastal areas during CEWCOM-78. NRL Technical Memorandum Report 3941, Mar. 1979. UNCLASSIFIED

32. Larson, R. E., D. J. Bressan, 1980: Air mass characteristics over coastal areas as determined by radon measurements. Second conference on Coastal Meteorology, Los Angeles, CA., Jan. 30-Feb. 1, 1980. UNCLASSIFIED

33. Larson, R. E., and R. K. Jeck, 1981: Atmospheric 222 Rn measurements at San Nicolas Island during 1980. NRL Technical Memorandum Report 4649, Oct. 1981. UNCLASSIFIED

34. Pearson, J. E., and G. E. Jones, 1965: Emanation of radon 222 from soils and its use as a tracer. J. Geophys. Res., 70, 5279-5290. UNCLASSIFIED

35. Clements, W. E., and M. H. Wilkening, 1974: Atmospheric pressure effects on 222 Rn transport across the earth-air interface. J. Geophys. Res., 79, 5025-5029. UNCLASSIFIED

36. Wilkening, M. H., 1974: Radon-222 from the island of Hawaii: deep soils are more important than lava fields or volcanoes. Science, 183, 413-415. UNCLASSIFIED

37. Larson, R. E., 1973: Measurements of radioactive aerosols using thin plastic scintillators. Nucl. Instrum. Methods., 108, 467-470. UNCLASSIFIED

38. Larson, R. E., and D. J. Bressan, 1978: Automatic radon counter for continual operation. Rev. Sci. Instru., 49, 965-969. UNCLASSIFIED

39. Shapiro, M. H., R. Kosowski, and D. A. Jones, 1978: Radon series disequilibrium in southern California coastal air. J. Geophy. Res., 83, 929-933. UNCLASSIFIED

40. Larson, R. E., 1979a: *Comment on 'Radon series disequilibrium in southern California coastal air' by M. H. Shapiro et al.* J. Geophys. Res., 84, 751. UNCLASSIFIED

41. Gat, J. R., G. Assaf, and A. Miko, 1966: Disequilibrium between the shortlived radon daughter products in the lower atmosphere resulting from their washout by rain. J. Geophys. Res., 71, 1525-1535. UNCLASSIFIED

42. Barnes, S. L., 1973: Mesoscale objective map analysis using weighted time series observations. NOAA Technical Memorandum ERL NSSL-62, Mar. 1973. UNCLASSIFIED

43. Cressman, G. P., 1959: An operational objective analysis system. Mon. Wea. Rev., 87, 367-374. UNCLASSIFIED

44. Brandes, E. A., 1976: Hourly surface weather maps and analyzed fields of meteorological variables. NOAA Technical Memorandum ERL NSSL-80, Dec. 1976. UNCLASSIFIED

45. Samson, P. J., 1980: Trajectory analysis of summertime sulfate concentrations in the Northeastern United States. J. Appl. Meteor., 19, 1382-1394. UNCLASSIFIED

46. Jacobi, W., and K. Andre, 1963: The vertical distribution of Radon 222, Radon 220 and their decay products in the atmosphere. J. Geophys. Res., 68, 3799-3814. UNCLASSIFIED

47. Larson, R. E., and W. A. Hoppel, 1973: Radon 222 measurements below 4 Km as related to atmospheric convection. Pageoph., 105, 900-906. UNCLASSIFIED

48. Larson, R. E., D. J. Bressan, and P. E. Wilkniss, 1982: Atmospheric measurements by the Atmospheric Physics and Chemical Oceanography Branches. NRL report in press, 1982. UNCLASSIFIED

INITIAL DISTRIBUTION

EXTERNAL	Copies
Commander	
Naval Air Systems Command Headquarters	
Attn: AIR-00D4	2
AIR-06	1
AIR-03P2 (J. Malloy)	1
AIR-370 (CAPT Ford)	2
(P. Twitchell)	
AIR-5332 (W. Whiting)	1
AIR-5333 (E. Cosgrove)	1
AIR-53631F (D. Caldwell)	1
Washington, DC 20361	
Defense Technical Information Center	
Cameron Station	
Attn: DDA	2
Alexandria, VA 22314	
Pacific Missile Test Center Liaison Office	
Naval Air Systems Command	
Attn: Liaison Officer	1
JP-2, Room 608	
Washington, DC 20361	
Commander	
Naval Material Command	
Attn: Code 08T22 (O. Remson)	1
Code 08T2211 (CDR Key)	1
Code 08T245 (G. Spalding)	1
Washington, DC 20360	
Commander	
Naval Electronic Systems Command	
Attn: ELEX-03G (R. Golding)	1
PME-107 (J. Obrian)	1
PME-107-52 (A. Ritter)	1
Washington, DC 20380	
Commander	
Naval Sea Systems Command	
Attn: Code 03415 (T. Tasaka)	1
NAVSEA-03 (S. Marcus)	1
PMS-405M	1
Washington, DC 20362	
Director	
Office of Naval Research	
Attn: Code 465 (J. Hughes)	1
800 N. Quincy	
Arlington, VA 22217	

EXTERNAL	Copies
Naval Surface Weapons Center	
Attn: CR-42 (Dr. B. Katz)	1
Code 213 (A. Hirshman)	1
Silver Spring, MD 20910	
Director	
Naval Research Laboratory	
Attn: Code 4326 (J. Fitzgerald)	1
Code 4327 (S. Gathman)	1
(R. Jeck)	1
Code 6560 (Dr. P. Ulrich)	1
Code 6567 (Dr. L. Ruhnke)	1
(G. Trusty)	1
(J. Dowling)	1
(T. Blanc)	1
Code 6754 (E. Alexander)	1
Code 8326 (Dr. R. Larson)	1
Washington, DC 20375	
Institute for Defense Analysis	
Attn: L. Biberman	1
H. Wolfard	1
W. Holzer	1
400 Army-Navy Drive	
Arlington, VA 22202	
Chief of Naval Operations	
The Pentagon	
Attn: CNO-35E (CAPT Pellock)	1
(L. Triggs)	1
Washington, DC 20350	
Commanding Officer	
Naval Intelligence Support Center	
Attn: NISC-40 (P. Roberts)	1
NISC-50 (R. Nelson)	1
4301 Suitland Road	
Washington, DC 20390	
Office of Asst. Secretary of the Navy	
(Research, Engineering & Systems)	
Department of the Navy	
Attn: H. Wang	1
Washington, DC 20350	
Office of Under Secretary of Defense	
(Research & Engineering)	
The Pentagon	
Attn: EPS (Room 3D1079, S. Musa)	1
E & LS (Room 3D129, COL Friday)	1
Washington, DC 20301	

EXTERNAL	Copies
Commander	
Air Force Armaments Laboratory	
Attn: AFAL/RWI-3 (CAPT W. Smith)	1
WRP-1 (R. Sanderson)	1
Wright-Patterson AFB, OH 45333	
Commander	
Naval Weapons Center	
Attn: Code 3918 (Dr. A. Shlanta)	1
(J. Stillwell)	1
Code 39042 (Dr. L. Wilkins)	1
Code 39403 (S. Breil)	1
(Dr. J. Wunderlich)	1
Code 39404 (S. Smith)	1
Code 3941 (D. Kummer)	1
Code 343 (Technical Library)	1
China Lake, CA 93555	
Commander	
Naval Ocean Systems Center	
Attn: Code 532 (Dr. J. Richter)	2
(D. Jensen)	1
(H. Hughes)	1
(R. Noonkester)	1
San Diego, CA 92152	
Commander	
USAF Air Development Test Center	
Attn: DLMT (M. Gay)	1
Eglin AFB, FL 32542	
Commander	
U.S. Air Force Geophysics Laboratory	
Attn: OPI (Dr. R. McClatchey)	1
OPM (Dr. R. Fenn)	1
OPR (B. Sanford)	1
Hanscom AFB	
Bedford, MA 01730	
David Taylor Naval Ship R&D Center	
Annapolis Laboratory	
Attn: Code 2833 (R. Burns)	1
Annapolis, MD 21402	
Defense Advanced Research Projects Agency	
1400 Wilson Blvd.	
Attn: S. Zakanycz	1
Arlington, VA 22209	

EXTERNAL	Copies
U.S. Army Electronics Research & Development Command, Atmospheric Sciences Laboratory	
Attn: DELAS-EO-MO (Dr. R. Gomez)	1
DELAS-EO-MO-ERADCOM (T. Hall)	1
DELAS-AS-T (R. Bonner)	1
(H. Holt)	1
White Sands Missile Range, NM 88802	
Commanding Officer	
Night Vision & Electro-Optics Laboratory	
Attn: DELNV-VI (Dr. R. Bergeman)	1
DRSEL-NV-VI (R. Moulton)	1
Fort Belvoir, VA 22060	
Commanding Officer	
Naval Environmental Prediction Research Facility	
Attn: Dr. A. Weinstein	1
Dr. A. Goroch	1
Mr. R. Fett	1
R. Nagle	1
Monterey, CA 93940	
Superintendent	
Naval Postgraduate School	
Attn: Code 62 CR (A. Cooper)	1
Code 61 CT (E. Crittenden)	1
Code 62 SG (G. Schacher)	1
Code 63 DS (K. Davidson)	1
Monterey, CA 93940	
Commander	
U.S. Army Missile Research Laboratory	
Advanced Sensors Directorate	
Attn: DRDMI-TEI (H. Jackson)	1
Redstone Arsenal, AL 35809	
Massachusetts Institute of Technology	
Lincoln Laboratory	
P.O. Box 73	
Attn: Dr. Kleiman	1
Lexington, MA 02173	
Grumman Aerospace Corporation	
Research Department	
Attn: J. Selby	1
Bethpage, NY 11743	
Scientific Technology Associates, Inc.	
Attn: S. Fishburn	1
Princeton, NJ 08540	

EXTERNAL	Copies
Environmental Research Institute of Michigan P.O. Box 8618 Attn: R. Legault Ann Arbor, MI 48107	1
Systems Planning Corporation 1500 Wilson Blvd. Attn: Dr. Friedman Arlington, VA 22209	1
General Research Corporation SWL Division 7929 Jones Branch Drive Attn: R. Rollins McLean, VA 22101	1
Northrop Corporation Aircraft Group 3901 West Broadway Attn: L. Tanabe Hawthorne, CA 90250	1

INTERNAL	Copies
Commander PACMISTESTCEN	
Code 0000	
RADM J. B. Wilkinson	1
Technical Director	
Code 0002	
K. I. Lichti	1
Project Management Group	
Code 0100	
CAPT B. L. Munger	1
Code 0141-2	
C. Elliott	1
Archive/Distribution Division	
Code 0334-1	
M. F. Hayes	10
Systems Evaluation Directorate	
Code 1001	
CAPT D. R. Laack	1
Technical Reports Library	
Code 1210-1	
(Bldg. 36)	2
Electromagnetic Systems Division	
Code 1230	
M. R. Marson	1
Code 1232	
D. T. Stowell	1
A. A. Akkerman	1
G. B. Matthews	1
Fleet Weapons Engineering Directorate	
Code 2001	
CAPT R. J. Miller	1
Range Directorate	
Code 3001	
CAPT J. M. Hickerson	1
W. L. Miller	1
Code 3210	
F. D. Roth	1
Measurement Systems Development Division	
Code 3140	
M. Bondelid	1
J. Loos	1

INTERNAL	Copies
Range Operations Department	
Code 3200	
CAPT R. L. Waters	1
Geophysics Division	
Code 3250	
CDR R. B. Glaes	1
D. A. Lea	1
Code 3251	
AGC M. A. Branaan	1
Code 3252	
B. R. Hixon	1
Code 3253	
J. S. Rosenthal	1
R. A. Helvey	1
T. E. Battalino	20
R. L. Clark	1
Code 3254	
M. J. Burkhardt	1
T. E. Hall	1
M. B. Bahu	1
C. D. Jacobs	1
Code 3280	
D. Tolzin	1
Naval Air Station	
Code 6001	
CAPT J. M. Tallman	1
Patent Counsel	
Code PC	
Dr. J. M. St. Amand	1


2-8
DT